UNIVERSITA' DEGLI STUDI DI CATANIA

DOTTORATO DI RICERCA
IN SCIENZE BIOCHIMICHE E BIOMOLECOLARI
XXIV CICLO

Site-directed mutagenesis and molecular modeling studies of h5-HT$_{7(a)}$ receptor reveal important residues for binding and activation

Tesi di Dottorato

Dottorando:
Dr.ssa Agata Antonina Rita Impellizzeri

Tutor:
Chir.ma Prof.ssa Angela Messina
Coordinatore:
Chiar.mo Prof. Angelo Vanella

TRIENNIO ACCADEMICO 2008-2011

TABLE OF CONTENTS

1 INTRODUCTION

1.1 Serotonin

Serotonin (5-hydroxytriptamine, 5-HT) is a physiologically active amine formed from the amino acid L-tryptophan by hydroxylation of the indole ring at C-5 and amino acid decarboxylation. 5-HT is degraded through oxidative deamination catalyzed by monoamine oxidase and subsequent oxidation to 5-hydroxyindoleacetic acid (5-HIAA).

Serotonin occurs in a wide variety of tissues throughout the body of mammals, but over 90% of 5-HT is found in enterochromaffin cells in the gastrointestinal tract, where it is synthesized and stored. 5-HT in the circulation is taken up through an active transport mechanism and stored in platelets. Serotonin is also synthesized and released by neurons in the CNS. The cell bodies of the all serotoninergic neurons in the CNS are localized in raphe nuclei. Serotoninergic peripheral neurons are found throughout various tissues and organs, including heart, kidney, lungs, spleen, gastrointestinal tractus and around blood vessels.

Serotonin is a neurotransmitter and a vasoactive hormone involved in the regulation of a wide variety of physiological and pathological processes. In the CNS serotoninergic neurons are involved in learning and memory, mood, sleep, temperature regulation, perception of pain and regulation of blood pressure and several psychiatric disorders, such as schizophrenia and depression (Hoyer et al. 2002).

Serotonin has diverse effects on the cardiovascular system, causing vasodilatation or vasoconstriction, depending on the vessel site and the condition of its intimal wall. In the heart it mediates cardioexcitation and cardiodepression (Kaumann and Levy 2006), this is probably mediated through excitation of sensory afferent vagal nerve endings. Platelets are regarded as the major source of circulating serotonin, which directly interacts with the cardiovascular system (Frishman and Grewall, 2000).

1.1.1 Classification of 5-HT receptors

Serotonin receptors are grouped into seven classes ($5-HT_{1-7}$) with 14 different subtypes, each encoded by a separate gene, where RNA editing and alternative splicing give additional receptor complexity (Heidmann et al. 1997). All mammalian serotonin receptors are GPCRs(G protein-coupled receptor) with the exception of the ligand-gated ion channel $5-HT_3$ (Hoyer et al. 1994). The major signal transduction pathway for the various subtypes are inhibition of Adenylyl Cyclase through G_i ($5-HT_1$), stimulation of phospholipase C (PLC) through G_q ($5-HT_2$) and stimulation of Adenylyl Cyclase through G_s ($5-HT_4$, $5-HT_6$, $5-HT_7$). The $5-HT_5$ receptor remains poorly characterized (Hoyer et al. 1994; Hoyer et al. 2002).

Family	Type	Mechanism	Effect
$5-HT_1$	G_i/G_o-protein coupled.	Decreasing cellular levels of cAMP.	Inhibitory
$5-HT_2$	G_q/G_{11}-protein coupled.	Increasing cellular levels of IP_3 and DAG.	Excitatory
$5-HT_3$	Ligand-gated Na^+ and K^+ cation channel.	Depolarizing plasma membrane.	Excitatory
$5-HT_4$	G_s-protein coupled.	Increasing cellular levels of cAMP.	Excitatory
$5-HT_5$	G_i/G_o-protein coupled.	Decreasing cellular levels of cAMP.	Inhibitory
$5-HT_6$	G_s-protein coupled.	Increasing cellular levels of cAMP.	Excitatory
$5-HT_7$	G_s-protein coupled.	Increasing cellular levels of cAMP.	Excitatory

Table 1: Classification of 5-HT receptors

1.1.2 The 5-HT$_7$ receptor

The 5-HT$_7$ receptor is the most recently described and cloned G$_s$ coupled receptor (Ruat et al. 1993). Three splice variants have been described in human (a, b and d) and in mouse (a, b and c) and four in rat (a, b, c and e) (Gellynck et al. 2008). Two isoforms are homologous in mouse, rat and human; they are designed 5-HT$_{7(a)}$ and 5-HT$_{7(b)}$ and are caused by two alternative donor sites located in tandem at the end of exon II. The use of the second splice donor site in the isoform 5-HT$_{7(b)}$ results in a 5bp insertion within the coding sequence, which introduces an in-frame stop codon. This shortens the C-terminal tail by 13 amino acids compared to the 5-HT$_{7(a)}$. The h5-HT$_{7(d)}$ contains an extra 98bp exon cassette at the exonII-exonIII boundary (Gellynck et al. 2008; Heidmann et al. 1997). In rat, a similar, yet distinct, exon (named exon C) provides the 5-HT$_{7(c)}$ splice variant (fig.1). The different splice variants in each organism differ only in the length and sequence of theirs carboxy-terminal tail and in the number of phosphorylation sites (Vanhoenacker et al. 2000).
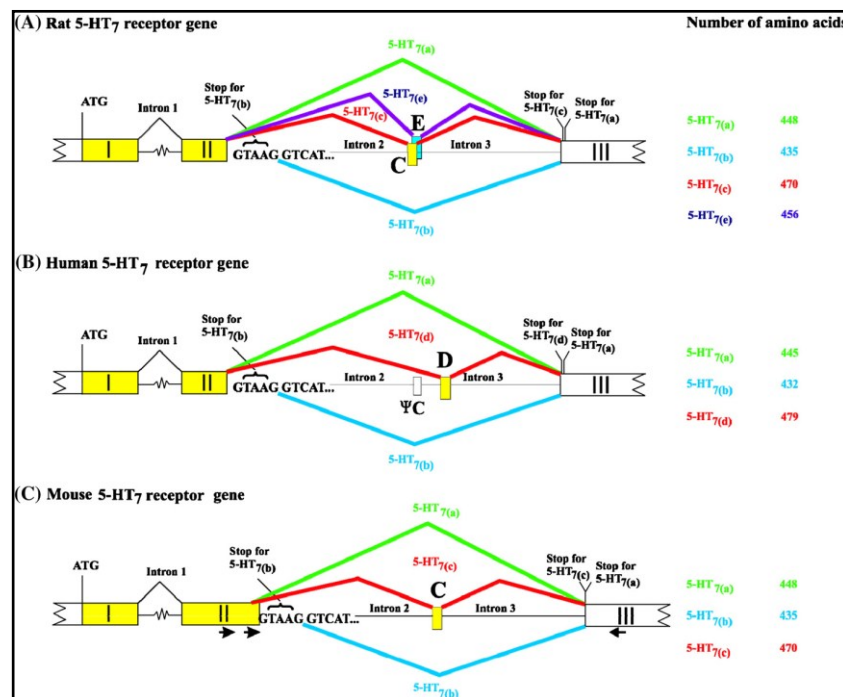

Fig1: 5-HT$_7$ receptor splice variants in rat, human and mouse.

The human isoforms $5-HT_{7(a)}$ and $5-HT_{7(b)}$ are present in brain, heart, kidney, liver, lung, placenta, small intestine, skeletal muscle, colon, ovary, testis, prostate, spleen and thymus tissues without difference in their relative abundance, with exception of $5-HT_{7(b)}$ receptors not being present in the colon, whereas $5-HT_{7(d)}$ receptor was not detected in kidney, skeletal muscle, prostate, thymus and it has lower expression in the other tissues than $5-HT_{7(a)}$ and $5-HT_{7(b)}$ receptors (Krobert et al. 2001). The $5-HT_{7(b)}$ receptor variant is the most expressed of all variants in the hypothalamus, and $5-HT_{7(d)}$ receptor is the least frequently expressed isoform and is mostly present in smooth muscle (Guthrie et al. 2005; Heidmann et al. 1997).

The presence of $5-HT_7$ receptors in the hypothalamus correlates with the possible involvement in thermoregulation, circadian rhythm, memory, activation of rapid-eye-movement (REM) sleep, endocrine regulation and hippocampal signaling; a possible involvement in regulation of mood suggest that $5-HT_7$ is a potential target for the treatment of depression (Hedlund and Sutcliffe 2004; Vanhoenacker et al. 2000; Gellynck et al. 2008).

All variants displayed identical G protein, Adenylyl Cyclase (AC) coupling and high affinity for 5-HT; this similar pharmacological profile and binding abilities show that the difference in the C-tail does not influence ligand binding or receptor activation (Krobert et al. 2001). Additionally they were constitutively active and displayed identical responses to constitutive AC activity. $5-HT_7$ receptors also behave as if they are pre-associated with G protein in the absence of ligand (Krobert et al. 2006). An exception is the $5-HT_{7(d)}$ receptor which displays a diminished 5-HT-stimulation of AC activity, due to constitutive internalization in an agonist-independent way (Krobert et al. 2001).

Other effectors of $5-HT_7$ were demonstrated in $5-HT_{7(a)}$. A recent study using mouse and insect cells reported that the mouse $5-HT_{7(a)}$ receptors couple to and activate G_{12}, resulting in transcriptional activation and regulation of cell morphology through Rho family small GTPases (Kvachnina et al. 2005). $5-HT_7$ receptors increase Ca^{2+} (Norum et al. 2005; Baker et al. 1998) which also increase activity of Ca^{2+}-responsive ACs (Baker et al. 1998).

Splice variants only differ in regulation of down-regulation, internalization and degradation: this is due to the difference in the C-tail which could mediate specific

interaction with trafficking pathway (Guthrie et al. 2005). The C-tail of 5-HT$_7$ receptors has been shown to specifically interact with intracellular proteins, such as the PLAC-24 protein, which might be involved in the transport of newly synthesized 5-HT$_7$ receptor towards the plasma membrane (De Martelaere et al. 2007a). In addiction it has been demonstrated that the C-terminus of mouse 5-HT$_{7(a)}$ receptor is dynamically regulated by palmitoylation, increased by agonist stimulation. C-terminal cysteine residues 404 and 438/441represent main palmitoylation sites and mutations in these sites increase the agonist-independent G$_s$ constitutive receptor activity (Kvachnina et al. 2009). 5-HT$_7$ has two YXXΦ motifs, 394YRSL and 402YRNI which could be implicated in regulating internalization (Paing et al. 2004; Paing et al. 2006), recruitment of GASP and SNX1 and thereby lysosomal targeting (Simonin et al. 2004; Moore et al. 2007). In addition, the 5-HT$_7$ receptor has recently been proposed to exist as a homodimer (Teitler et al. 2010).

Most atypical and some typical antipsychotic drugs bind to 5-HT$_7$ receptors and have been suggested to be involved in treatment of pain, schizophrenia, anxiety, cognitive disturbances and inflammation (Gellynck et al. 2008). Numerous serotoninergic antagonists (methiothepin, clozapine, ketanserin, spiperone, metergoline, methylsergide and mesulergine) display different agonist properties at the 5-HT$_7$receptor, varying among neutral antagonist, partial inverse agonist and weak partial agonist (Roth et al. 1994; Krobert and Levy 2002). Clozapine is an atypical antipsychotic with high affinity for 5-HT$_7$receptors which behaves as an inverse agonist when measuring Adenylyl Cyclase activity (Roth et al. 1994). Additionally, 5-HT$_7$ receptor can be pseudo-irreversibly blocked and thus inactivated by some ligands, such as methiothepin and the atypical antipsychotic risperidone (Smith et al. 2006; Krobert et al. 2006).

1.2 G-protein-coupled receptors

1.2.1 Structure and classification of G protein coupled receptors

G-protein-coupled receptors (GPCRs) represent a broad class of cell surface receptors that transduce the effects of diverse signal molecules, including photons, organic odorants, nucleotides, nucleosides, peptides, lipids and proteins to intracellular

signalling pathways through the activation of heterotrimeric G proteins. GPCRs represent the largest and most diverse superfamily of proteins in the whole human body with over 100 subfamilies, according to the sequence homology, ligand structure and receptor function (Ji et al. 1998).

The general structure of all GPCRs show an extracellular N-terminal segment, seven transmembrane (TM) spanning-α-helical domain, which form the TM core, composed of 20-27 aminoacids, three extracellular loops (exoloop), three intracellular loop (citoloop) and an intracellular C-terminal segment. The C-tail can be palmitoylatedat a cysteine residue, thus forming a fourth-cytoloop anchored to the plasma membrane (fig.2) (Ji et al. 1998). The TM core is tightly packed by hydrogen bonds and salt bridges, leaving no room for a channel or tunnel structure (Ji et al. 1998). The TMs 1, 4, 7 are significantly more hydrophobic than TMs 2, 3, 5, 6, which contain ionic and neutral residues. TM 3 is believed to be the preliminary site for ligand binding whereas TMs 5 and 6 are the signal generation site.
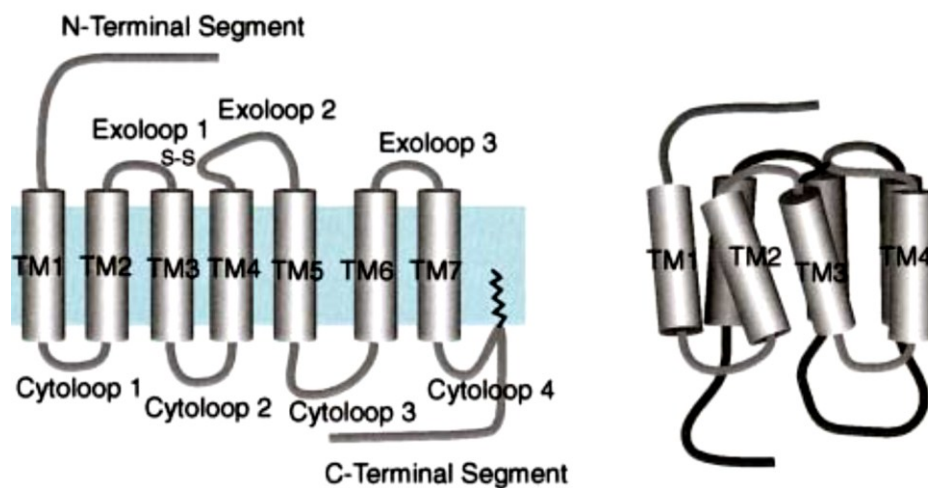

Fig. 2: Schematic presentation of the general structure of GPCRs in a planar and three dimensional views.

Based on sequence similarity GPCRs are grouped in three main families, where each family shares more than 25 % of sequence identity in the transmembrane core region and highly conserved motifs. Family 1 is the most studied and includes family 1a with receptor for rhodopsin and receptors for small molecular weight ligand (such as adrenalin and serotonin), family 1b for peptide receptors which bind to the N-terminus and exterior parts of TMs, family 1c for glycoprotein receptors. Family 2 GPCRs have similar morphology to group 1c, but do not share any sequence homology. Their ligands include high molecular weight hormones, such as glucagon and calcitonin. Family 3 is related to the metabotropic and Ca2+ sensing receptors. Family 4 includes pheromone receptors and family 5 includes receptors involved in embryonic development (Bockaert and Pin 1999).

1.2.2 Heterotrimeric G proteins

G proteins are members of a superfamily of GTPases that play diverse roles in many aspects of cell regulation. There is a structural and functional diversity between the three polypeptide subunits (an α-subunit and a dimericβγ-subunit) components of a G protein heterotrimeric (Pierce et al. 2002).

All types of heterotrimeric G proteins are activated by a common mechanism (fig. 3). In the inactive state α-subunit is bound by GDP and receptor activation induces a conformation change which activates G proteins by releasing GDP from the nucleotide binding pocket of G_α. Release of GDP is followed by GTP binding, which promotes the dissociation of the heterotrimer into an α-subunit and a dimeric βγ-subunit. Both these subunits regulate the activation and inhibition of different G-protein-coupled effectors. G_α subunit has an intrinsic GTPaseactivity which hydrolyses a phosphate group of GTP and leaves GDP in the nucleotide binding pocket, which allows the re-association of the G_α-GDP with $G_{\beta\gamma}$ for a new cycle (Milligan and Kostenis 2006; Pierce et al. 2002; Cabrera-Vera et al. 2003).
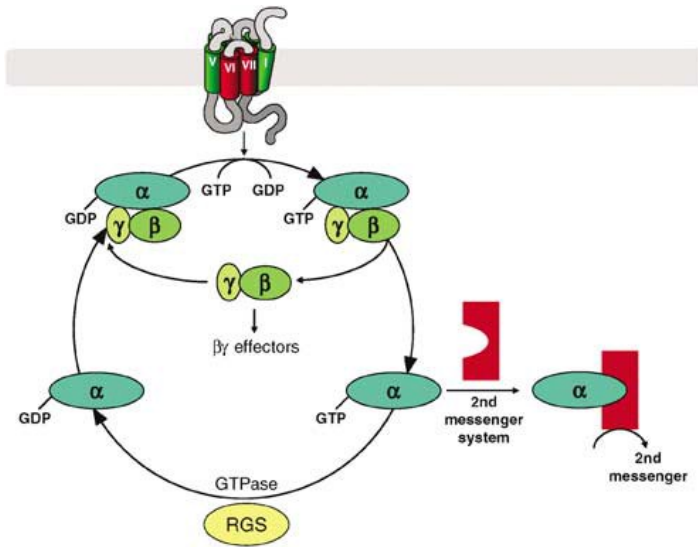
Fig. 3: Mechanism of G protein. Conversion of G protein heterotrimeric inactive state with GDP-G_α to active state GTP-G_α and dissociation to heterotrimeric in G_α and $G_{\beta\gamma}$ which regulate several effectors.

Heterotrimeric G proteins have been highly conserved during the evolution. There are four principal G protein families (G_s, G_i, $G_{q/11}$ and $G_{12/13}$), each identified by aminoacid similarities and α-subunits that preferentially regulate specific classes of effectors: G_s-family stimulates adenylyl cyclase (AC); G_i-family ($G_{\alpha o-1-2}$, $G_{\alpha i-1-3}$, $G_{\alpha oA-B}$, $G_{\alpha z}$, $G_{\alpha g}$) is implicated in regulation of ion channel activity, inhibition of AC and regulation of phospholipase C (PLC); $G_{q/11}$- family ($G_{\alpha 11,14-16}$ and $G_{\alpha q}$)regulates the activation of phosphoinositide-specific PLC (PLC-β); $G_{12/13}$ family activates small GTP binding G proteins (Rho, Rac and Cdc42) (Milligan and Kostenis 2006; Kvachnina et al. 2005).

The β and γ subunits are tightly associated through a coiled-coil structure and are functionally regarded as a monomer. Five distinct members of the G_β-family (β1-5) and twelve members of the G_γ-family (γ1-12) have been identified. The $G_{\beta\gamma}$ subunits are able to activate ion channel (K^+ and Ca^{2+} channels), PLA2, PLC, AC, GPCR kinase (GRKs) and phosphoinositide kinase (PI3K) (Milligan and Kostenis 2006; Cabrera-Vera et al. 2003).

G proteins are regulated by regulators of G protein signalling (RGS) which lead to termination of the cycle by hydrolysis of GTP to GDP with following reassociation of the heterotrimer, while adenylyl cyclase enhances the GTPase activity of G_s-subunits (fig. 4) (Pierce et al. 2002; Milligan and Kostenis 2006).
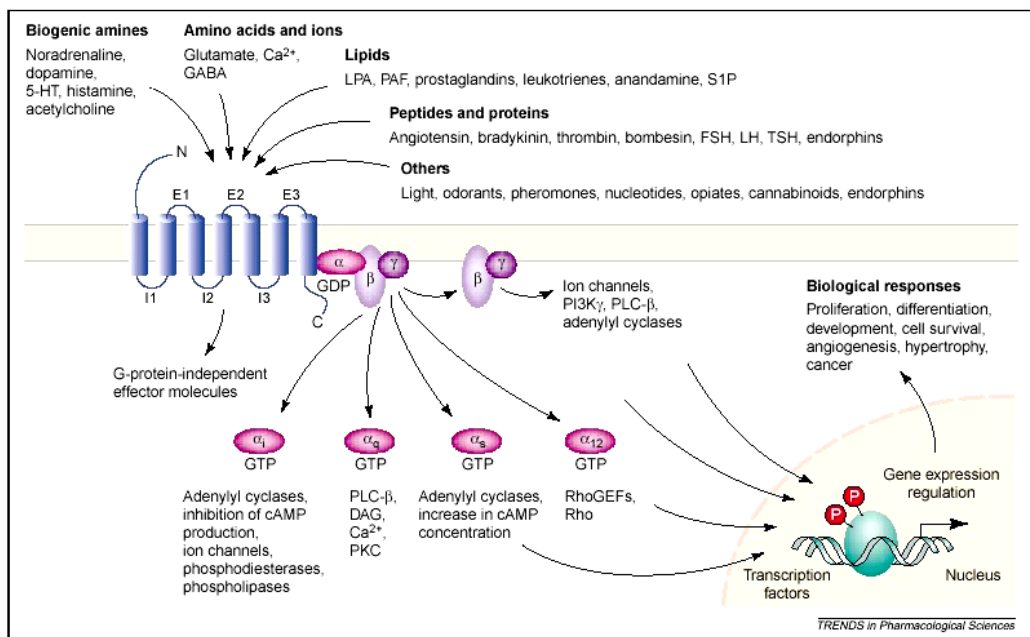

Fig. 4: G-protein families and their specific classes of effectors

1.3 GPCR signal transduction

1.3.1 Ligand binding

In the interaction between ligand and receptor seems to be involved hydrogen bonds, ion pairs, and hydrophobic interactions. Ligands are characterized by both the affinity for the receptor (potency, capacity of ligand to bind the receptors), and the efficacy (the property of ligands to induce a receptor response) (Urban et al. 2007). Several distinct modes have been observed for high affinity ligand binding to GPCRs. These can be grouped according to the nature of the ligand and the receptor. Small molecules weight ligands, such as amines, nucleotides, eicosanoids and lipid moieties bind to the TM core (cavity formed by TM3 to TM6), generating a conformational change. Peptides bind to both the core and exoloops. Polypeptides bind to both exoloops and N-terminal segment, whereas glycoproteins bind exclusively to the N-terminal segment. Small neurotransmitters such as glutamate and GABA, as well as Ca^{2+} bind to the N-terminal segment.

Ligands, which bind to the N-terminal segment, activate the receptor when the N-terminal segment complex undergoes a conformational change, which leads to a secondary contact between the liganded N-terminal and the exoloops, thus generating a TM signal (Ji et al. 1998; Bockaert and Pin 1999).

GPCRs are activated by ligand by conformational change that alter the core formed by TM3 and TM6 to expose G protein binding site in cytoloop 2 and 3 (Gether and Kobilka 1998). Diverse ligand-binding lead, differently, receptors to G-protein activation, internalization, desensitization, oligomerization, phosphorilation and dissociation from other proteins (Kenakin 2002).

Costa and Herz demonstrated for the first time the existence of antagonists with negative intrinsinc activity, where ligands decrease the basal activity of the receptor system, activated in absence of agonists; this effect was defined as inverse agonism (Costa and Herz 1989). In addition, long exposition of inverse agonist is associated with upregulation of the receptor involved or can have effects on other receptor systems (Seifert and Wenzel-Seifert 2002). Some inverse agonists are used as drugs in the clinic

with important therapeutic action, like cimetidine, haloperidol, prazosin, timolol and clozapine(Strange 2002).

1.3.2 Model for receptor activation

In classical GPCR theories, agonist binding to the receptor is necessary to induce a change in receptor conformation which would activate the G protein (Strange 2002). Later discoveries demonstrated that many GPCRs display constitutive activity which is abolished by inverse agonists, which resulted in the proposal of the two-state model where receptors are in equilibrium between inactive R and active R* conformation, promoted by inverse agonists and agonist, respectively. GPCRs in R state are uncoupled from G protein and in R* state are coupled to and activates G protein, as shown in fig.5 (de Ligt et al. 2000). This isomerization can also occur independent of ligands, which results in constitutive GPCR activity (Seifert and Wenzel-Seifert 2002). Other models were presented to describe activation of GPCRs as the ternary complex model (De Lean et al. 1980; Samama et al. 1993), where the interaction between agonist, receptor and G-protein is considered, and the extended ternary complex model, which is a combination of the first two models (Galadrin et al. 2007). This extension has been termed the cubic ternary complex model (Weiss et al. 1996).

Receptor ligands can be classified in three categories: i) full agonists with high efficacy and high affinity for the R* state; ii) full inverse agonists which maximally stabilize the R state; iii) neutral antagonists which do not affect the equilibrium but block the effects of agonist and inverse agonists, or as partial agonists and partial inverse agonists which have lower efficacy than full agonists and full inverse agonists. The constitutive GPCR activity defines the basal G protein and effectors activity, which is increased by agonists and decreased by inverse agonists, while antagonists do not have any effect (Seifert and Wenzel-Seifert 2002).
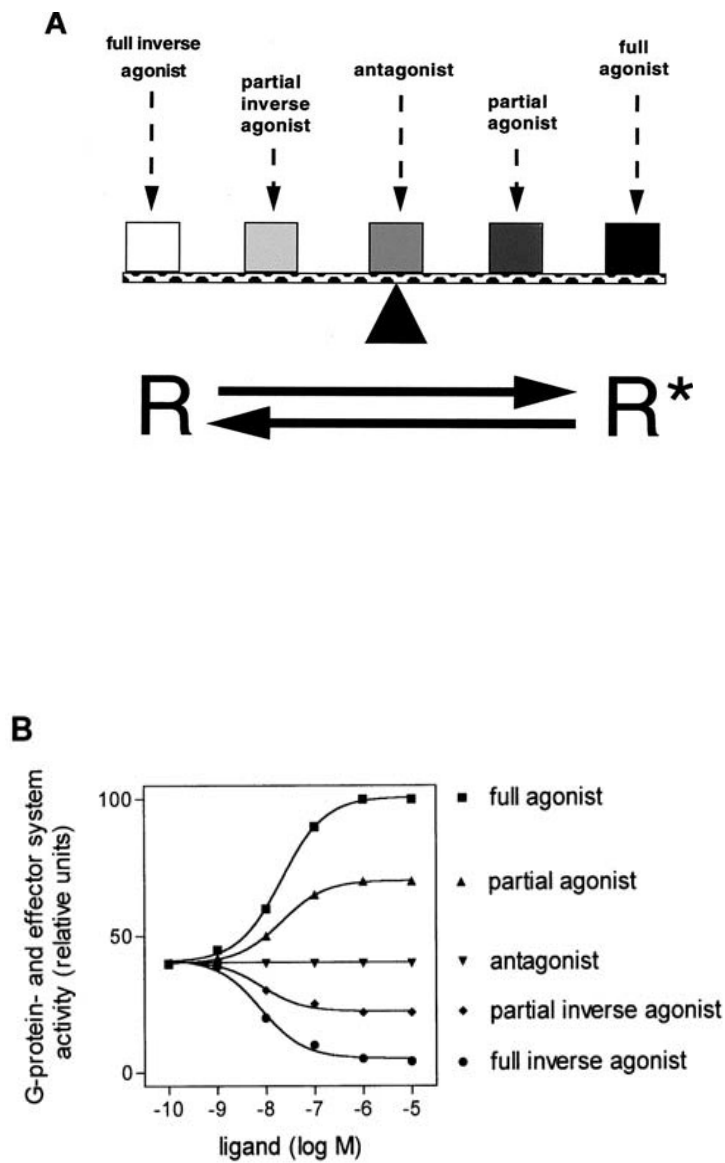
Fig.5: (A) The two-state model GPCR activation assumes that GPCRs isomerizes from an inactive (R) state to an active (R*) state. (B) Activity of effector systems R- to R* isomerization in GPCRs is referred to as constitutive activity. R* state promotes the exchange GDP/GTP at G proteins and regulate the activity of effectors.

15

1.3.3 Adenylyl cyclase

Adenylyl cyclase catalyses the conversion of ATP to cAMP, one of main second messenger of GPCR signalling (Tang and Hurley 1998). Many different types of agonist stimulated GPCRs are known to modulate the activity of the effector enzyme adenylyl cyclase through coupling to the G proteins G_s and G_i.

Nine transmembrane isoforms of AC have been cloned and characterized, but subsequently a soluble enzyme, sAC, which is not responsive to G-proteins or other regulators of the membrane-bound enzymes was discovered. They have different expression patterns in human and respond positively or negatively to distinct sets of regulatory inputs.

All ACs contain two large hydrophobic regions, predicted to consist of six transmembrane α-helices connected by relatively hydrophilic intra- and extracellular loops. The first six TMs are separated from the last six TMs by a quite long intracellular loop, giving ACs a constitution of two similarly organized halves. The two formed cytoplasmic domains share homology with each other and form a large catalytical domain. The presence of Mg^{2+} is necessary for the catalytic activity of AC (Hurley 1999). There is abundant kinetic evidence for a two-ion mechanism. One ion acts kinetically as free Mg^{2+}, whereas the other complexes with ATP, providing the true substrate for AC (Simonds 1999).

All ACs, except isoform 9, are stimulated by forskolin and activated by GTP-bound $G_{\alpha s}$ (Hurley 1999; Tang and Hurley 1998).

Active G proteins bind and induce a conformational change in AC which allosterically stimulates it. The $G_{\beta\gamma}$-subunit stimulates synergistically with $G_{\alpha s}$ certain types of AC, but inhibits others. Phosphorylation by protein kinases such as second messenger-regulated protein kinases PKA and PKC or Calmodulin kinase may lead to activation or inhibition of different isoforms of ACs (Simonds 1999; Hurley 1999).

The phosphodiesterase (PDE) family controls the intracellular level of cAMP by hydrolysis of cAMP into inactive AMP (Cooper 2003).

cAMP acts as a second messenger with key role in intracellular signalling pathways ofhormones, neurotransmitters, odorants and chemokines. The main effectors of cAMP are PKA and Epac. PKA is a tetramericholoenzyme, which phosphorylates

serine and threonine residues in the catalytic site of ACs, thereby reducing AC activity (Cooper 2003). Another target of cAMP is an exchange protein directly activated by cAMP (Epac), which functions as a guanine nucleotide exchange factor (GEF) for G proteins such as Rap,by catalyzing the exchange of GTP for GDP and consequently activation of G protein (Gloerich and Bos 2010).

2 METHODS

2.1 Preliminary homology model approach

The activity of a biological molecule, as every molecule, is strictly related to its structure. So far only four GPCR structures have been solved by high resolution X-ray crystallography: rhodopsin, β_2Adrenergic-Receptor, β_1Adrenergic-Receptor, A_{2A} adenosine receptor. It is more difficult obtaining X-ray structures of transmembrane proteins than globular ones; for this reason there is a lack of information about the structure of these receptors.

One method used to overcome the demand of structural information of proteins is *homology modeling or comparative modeling*, a knowledge-based method.

The homology modeling is based on the assumptions that the protein structure mainly depends on its primary structure and that among proteins the 3D structure is more conserved than proteins sequences. For this reason proteins that show different primary structure probably share common structural features and particularly the overall fold.

Thus it is possible to deduce a 3D structure of a protein from a template (or more). A template is a protein with known structure which has been selected for its high sequence similarity on respect to the target. The selection of the target is made by means of sequence alignment methods (pairwise sequence alignment, multi sequence alignment). The next step is the identification of conserved main chains from target-template comparison, then a pre-model is generated. A pre-model is a set of 3D coordinates of C_α in target main chains; these coordinates resemble the coordinates of the template backbone in domains aligned with the target.

Variable regions, identified by sequence alignment, are often modeled considering that loops generally possess similar length and amino acid character; therefore these features are structured considering coordinates of several template models.During the model generation side chains and loops conformations are chosen without restricted criteria; thus an energy refinement is necessary. Also crystal structures must be relaxed in order to remove internal strains resulting from the crystal packing forces. The energy minimization step must be run on the overall model.

Structure refinement could be obtained by molecular dynamics simulations running in several environment conditions: *vacuum*, water, membrane. For biological systems it is recommended to simulate cytosolic and membrane environments in order to generate *real life* models.

Molecular mechanics or molecular dynamics are mostly used to predict theconformational changes in the ligand-target binding process. Semi-empirical, *ab initio* quantum chemistry methods, or density functional theory are often used to provide optimized parameters for the molecular mechanics calculations and also provide an estimate of the electronic properties (electrostatic potential, polarizability, etc.) of the drug candidate which will influence binding affinity.

Molecular mechanics methods may also be used to provide semi-quantitative prediction of the binding affinity and to identify specific aminoacids involved in the binding interactions with the receptor.

2.2 Site-directed mutagenesis

Mutations in the human $5\text{-HT}_{7(a)}$ receptor are carried out using the QuikChange® Site-Directed Mutagenesis kit (Stratagene) by a PfuTurbo DNA polymerase and a thermal temperature cycler. The procedure utilizes a dsDNA (pcDNA3.1/CMV) with an insert (coding region of the $h5\text{-HT}_{7(a)}$) and two synthetic oligonucleotide primers each one about 25-30 bp,with a melting temperature (T_m) of $\geq$ 78 °C. The desired mutation (single point) should be in the middle of the primer with ~ 10-15 bases of correct sequence on both sides.

The oligonucleotide primers, each complementary to opposite strands of the vector, are extended during thernal cycling. The sample reaction is prepared as below:

- ✓ 5 µl of 10X reaction buffer
- ✓ 5-50 ng of dsDNA template
- ✓ 125 ng of oligonucleotide primer Forward
- ✓ 125 ng of oligonucleotide primer Reverse
- ✓ 1 µl of dNTP mix
- ✓ ddH$_2$O to a final volume of 50 µl
- ✓ 1 µl of *Pfu Turbo* DNA polymerase (2.5U/µl)

Each cycle reaction using the cycling parameters outlined in table 2

Cycles	Temperature	Time
1	95° C	1 minute
18	95° C	50 seconds
	60° C	1 minute
	68° C	1 minute/kb of plasmid length
1	68°C	7 minute

Table 2: cycling parameters

Following temperature cycling, the reaction mix is placed on ice for 2 minutes to cool the reaction to ≤ 37° C. Afterwards the reaction product is treated with 1μl of*DpnI*(10U/μl).The reaction mixture is gently mixed by pipetting the solution up and down several times. The reaction mixture is spinned down in a microcentrifuge for 1 minute and immediatelyis incubated at 37° C for 1 hour to digest the parental dsDNA template and to select the mutated dsDNA.

Before to proceed with the transformation protocol, the XL1-Blue supercompetent cells are thawed on ice. 1 μl of the *DpnI*-treated DNA is transferred in 50 μl of cells, the transformation reaction is gently mixed and is incubated on ice for 30 minutes. Afterwards the reaction is incubate for 45 seconds at 42° C and then the reaction is placed on ice for 2 minutes. 500 μl of LB medium is added to the reaction solution and it is incubated at 37° C for 1 hour with shaking at 225-250 rpm.

At the end the appropriate volume of transformation solution is plated on agar plate containing the specific antibiotic for the plasmid vector, and incubated at 37° C for > 16 hours.

2.3 Small-scale plasmid preparation

For small-scale isolation and purification of plasmids from transformed cells the Wizard® Plus SV Miniprep kit (Promega) is used.

2-10 ml of overnight bacterial culture isspinned down for 5 minutes at 14000 rpm in a tabletop centrifuge. The supernatant is discarded and added 250 µl of Cell Resuspension Solution (50 mMTris-HCl, pH 7.5, 10 mM EDTA, 100 µg/ml RNase A) to resuspend the cell pellet by vortexing.

250 µl of Cell Lysis Solution (0.2 M NaOH, 1 % SDS) is added and the solution is mixed by inverting the tubes 4 times. 10 µl of Alkaline Protease Solution is added to the lysate and mixed by inverting again. The solution is incubated for 5 minutes at room temperature. The alkaline protease inactivates endonucleases and other proteins released during the lysis of the bacterial cells that can adversely affect the quality of the isolated DNA.

350 µl of Neutralization Solution (4.09 M guanidine hydrochloride, 0.759 M potassium acetate, 2.12 M glacial acetic acid) is added to the reaction mixture and is mixed by inverting the tubes 4 times. The bacterial lysate is centrifuged at 14000 rpm for 10 minutes at room temperature.

The cleared lysate is transferred into the Spin Column inserted into a 2 ml collection tube by decanting. The supernatant is centrifuged at 14000 rpm for 1 minute at room temperature and the flowthrough is discarded from the collection tube. 750 µl of Column Wash Solution (60 % etanol v/v, 162.8 mM potassium acetate, 27.1 mMTris-HCl pH 7.5) is added to the column. The column is centrifugated for 1 minute at 14000 rpm and the flowthrough is discarded. The wash procedure is repeated with 250 µl of Column Wash Solution and the column is centrifugated again for 2 minutes at 14000 rpm at room temperature. The column is transferred to a sterile 1.5 ml tube and the DNA is eluted by adding 100 µl of Nuclease-Free Water to the Spin Column and is centrifugated for 1 minute at 14000 rpm at room temperature. The purified plasmid DNA is stored at -20° C.

2.4 DNA sequencing

The purified mutated plasmid DNA is analysed and confirmed by DNA sequencing. They are sequenced by ABI-lab using ABI 3730 DNA analyzershigh-throughput capillary electrophoresis machines.The reaction mix is performed using around 0.5-1.0 µg of DNA sample, 1 µl (10 µM) for each Forward and Reverse primers, 4.0 µl of Terminator ready Reaction Mix. The sequence reaction, using fluorescently labelled nucleotides in combination with a cycling PCR protocol. The cycle sequencing reaction were cycled 25 times for 10 seconds at 96° C, followed by 5 seconds at 50° C and 4 minutes at 60° C. The ABI BigDye Terminator sequencing buffer and v3.1 Cycle Sequencing kit are used. By indicating the optimal temperature for the primer in the delivery form, the annealing temperature will adjust accordingly, provided it is above 40° C and below 60° C.the reaction mix is spinned down in a microcentrifuge and prepared for the purifying procedure through capillary electrophoresis.

2.5 Transformation

After sequencing test the mutated plasmid are transformated in TOP 10 competent *E.coli* cells. They are highly sensitive to changes in temperature or mechanical lysis caused by pipetting. The cells are thawed on ice and immediately the transformation protocol should start.

1 µl of mutated plasmid DNA is added to 25 µl of competent TOP 10 cells and gently mixed together. The transformation mix is incubated on ice for 15 minutes. Afterwards the heat shock is performed and the cells are put at 42° C for 30 seconds without shaking and then are incubated immediately on ice for 2 minutes. 125 µl of room temperature SOC medium (20g/L tryptone, 5g/L yeast extract, 0.9 % NaCl, 10mM $MgCl_2$, 10 mM $MgSO_4$, 2.5 mM glucose) is added to the reaction mix and gently mixed. The reaction mix is incubated in a horizontal shaker at 37° C, 200 rpm for 30 minutes. 50- 100 µl of the transformation mixture is spread onto a LB plate (LB medium: 10 g/L Bacto-tryptone, 10 g/L NaCl, 5 g/L yeast extract, pH 7, 20 g/L Bacto-

agar for LB plates) containing 80 µg/ml ampicillin. The cells are incubated overnight in a horizontal shaker at 37° C.

To use the plasmid containing the desired mutation in other procedure, 4 colonies are picked and grown in 8 ml of LB medium for large-scale plasmid preparation.

2.6 Large-scale plasmid preparation

To produce larger amounts of purified plasmid DNA, large-scale plasmid preparation is set up using the Qiagen Plasmid maxi Kit (QIAGEN). The bacterial cells are lysed with a solution containing NaOH and SDS; upon neutralization and increasing the salt concentration, chromosomal DNA, cell membrane components and denatured proteins will precipitate, while plasmid DNA remains in solution. An alkaline protease is addedto inactivate endonucleases and to non-specifically degrade proteins. RNase A is added at the beginning of the procedure to digest the liberated RNA as to minimise RNA contamination. The lysate is run through an anion-exchange column consisting in silica beads with high density of diethylaminoethyl (DEAE) groups, these are positively charged in acidic environment and will interact with negatively charged molecules, such as phosphate groups on DNA and RNA. Washing with a medium-salt buffer will remove contaminants such as RNA and protein. Plasmid mutated DNA is eluted using a high-salt buffer, then it is desalted and concentrated by isopropanol precipitation.

2 ml of a starter cells culture are added to 500 ml LB medium containing 80 µg/ml of ampicillin and the culture is incubated at 37° C for 12-16 hours in a shaker incubator. The bacterial cells are centrifugated at 6000 g for 15 minutes at 4° C. All traces of supernatant are totally removed and the bacterial pellet is resuspended in 10 ml of buffer P1 (resuspension buffer: 50 mMTris-HCl, pH 8.0, 10 mM EDTA, 100 µg/ml RNase A). 10 ml of buffer P2 are added (lysis buffer: 200 mMNaOH, 1 % SDS w/v) and gently mixed by inverting the tube 4-5 times. The reaction mixture is incubated for 5 minutes at room temperature. Afterwards 10 ml of buffer P3 are added (neutralization buffer: 3.0 M potassium acetate, pH 5.5) and immediately mixed by inverting for 4-5 times. The lysate is poured into the capped barrel of QIA filter Cartridge and is incubated for 10 minutes at room temperature. A HiSpeed Maxi tip is equilibrated by applying 10 ml of buffer QBT (equilibration buffer: 750mM NaCl, 50 mM MOPS, pH

7.0, 15 % isopropanol, 0.15 % Triton®-X-100). Gently the plunger is inserted the QIA filter and the cell lysate filtered into the HiSpeed Maxi tip. The cleared lysate enters the resin by gravity flow, then the HiSpeed Maxi tip is washed with 60 ml buffer QC (wash buffer: 1.0 M NaCl, 50 mM MOPS ph 7.0, 1.5 mM isopropanol). The DNA is eluted with 15 ml of buffer QE (elution buffer: 1.25 M NaCl, 50 mMTris-HCl pH 8.5, 15 % isopropanol) and is precipitated by adding 10.5 ml of isopropanol. The solution is mixed and incubated at room temperature for 5 minutes. The eluate/isopropanol solution is filtered through a QIAprecipitator Maxi Module (membrane filter) attached to a 30 ml syringe and the flowthrough is discarded. The DNA is washed with 2 ml of 70 % of ethanol, the membrane filter is dryed by pressing air through the QIAprecipitator. This step is repeated 3 times. The QIAprecipitator is attached to a 5 ml syringe and the DNA is eluted into a 1.5 ml sterile tube by adding 1 ml of TE buffer (10mM Tris-HCl pH 8.0, 1 mM EDTA) and stored at -20° C.

2.7 Quantification of DNA

Quantification of DNA is performed by UV analysis. Nucleotide spectra are complex to analyse quantitatively because they have many non bonded electrons with indistinct transitions giving a multitude of absorption between 200 nm and 300 nm. All nucleotides however have a λ max near 260 nm which is fairly specific for the purine and pyrimidine bases. This wavelength can be used to estimate the nucleic acid concentration in a sample. DNA also absorbs light at 230 and 280 nm, but to a lesser extent. Pure DNA samples should have the following absorption ratios:

OD_{260}/OD_{280} ratio ~ 1.8-1.9

OD_{260}/OD_{230} ratio ~ 1.8-2.2

Asp, Glu, Asn, Gln and His side chains have adsorption in the region 190-230 nm, whereas aromatic amino acids, Phe, Tyr and Trp, absorb UV-light around 280 nm. Thus high absorbance at 230 nm indicates contamination by urea, phenol or proteins, whereas high absorbance at 280 nm denotes mainly protein contamination. Using OD_{260} to estimate concentration is only valid if the ratio are within their limits, otherwise the solution is not pure nucleic acid and the OD_{260} may include absorbance by other molecules. If the DNA sample follows these criteria, the total amount of DNA can be calculated using the following formula:

DNA (μg/μl)= OD_{260} X dilution/20

The spectrophotometer used to measure the OD's DNA concentration (Nanodrop 2000 UV/Visible aspectrophotometer, Thermo scientific) doesn't need instrumental adjustments but makes a simple self calibration before use. 2 μl of buffer TE are pipetted out for the blanks measurement and then 2 μl of samples are used to measure the concentration directly on the pedestal. When the measurement is complete, the surfaces are simply wiped before going on to the next sample. A specific Nanodrop2000 software shows the accurate concentration of the DNA samples.

2.8 Culturing QBI-HEK293 cell line

The obtained mutants are expressed in QBI-HEK293 cells. This cell line is an immortalized line of primary human embryonic kidney cells, subclone of HEK293 cells and strongly adheres to plastic dishes, performing extremely well in plaque assay and trasfection experiments. The human QBI-HEK293 cells are a good model system to study GPCRs, they contain human proteins, they grow fast and don't express any 5-HT receptor subtypes in their membrane. The QBI-HEK293 cells are grown in Dulbecco's modified Eagle's medium (DMEM; GIBCO) with 10% fetal bovine serum (BioWhittaker) and penicillin (100U/ml) and streptomycin (100μg/ml). Cells are transiently transfected with wild-type and mutated plasmid DNA (pcDNA3.1(-) containing h5-HT$_{7(a)}$) using a serum-free medium (ULTRAculture, BioWhittaker; because serum contains high concentration of serotonin) supplemented with L-glutamine (4mM) and penicillin (100U/ml) and streptomycin (100μg/ml). The transfection mix contains also LIPOFECTAMINE^{TM} – LTX reagent (Invitrogen^{TM}) and 7,5 μg DNA per 150 mm dish.

2.9 Splitting cells

The cells are split by trypsin-EDTA treatment whenever the culture dishes became 80-90% confluent. The DMEM medium is sucked out and the cells are washed once with 10 ml of sterile 0.9 % NaCl solution. Then 1 ml of trypsin-EDTA is added to cover the cells and incubate for 2 minutes at 37° C in a CO_2 incubator, afterwards 10 ml

of DMEM medium are added and the cells are transferred to a 15 ml sterile tube and are centrifugated at 2100 rpm for 5 minutes. The DMEM medium and the trypsin-EDTA are removed, the cells are resuspended with new medium considering a specific dilution and are kept at 37° C in a CO_2 incubator.

2.10 Transfection

Transfection is the process of deliberately introducing nucleic acids into eukaryotic cells. For eukaryotic cells, transfection is better achieved using cationic lipids (or mixtures), because the cells are more sensitive. In this study the Lypofectamine LTX (Invitrogen) reagent is used.

In a 150 mm tissue culture plate the cells are 60-70 % confluent in 10 ml of DMEM medium with 10 % FBS (fetal bovine serum), 100 U/ml penicillin and streptomycin (100μg/ml), while two specific solutions are performed:

solution A: 37,5 μl of Lipofectamina LTX (Invitrogen) + 375 μl of OptiMEM®
solution B: 7,5 μg of DNA + 375 μl of OptiMEM®

The two solution are gently mixed together and are incubated at room temperature for 30 minutes. During this time the cells are washed with 15 ml of NaCl or OptiMEM® and 12.5 ml of Ultraculture (serum free) containing 4 mM glutamine and 100 U/ml penicillin and 100μg/ml streptomycin are added to each plate. After 30 minutes the mixed solution A+B is added onto the washed cells, mixed gently by swirling the plate around. Then the cells are incubated overnight at 37° C/ 5% CO_2. After 24 hours the medium (Ultraculture-Gln-PS, BioWhittaker) is replaced and incubated again overnight. After 48 hours the membrane preparation are performed.

2.11 Membrane preparation

Membrane preparation from QBI-HEK293 cells are performed 48 hours after transfection. The cells should be ~ 70-80 % confluent to proceed with the membrane preparation procedure.

The transfection medium is sucked out and the cells are washed twice with 5 ml of ice cold HBBS (Hanks Balanced Salt Solution), then other 10 ml of HBBS are added

to the cells. Afterwards the cells are scraped with a plastic scraper and the solution containing the cells is transferred in a 15 ml tube. The cells are collected by centrifugation at 2100 rpm for 5 minutes at 4° C. The supernatant is discarded and the pellet is resuspended with 1 ml of STE buffer (27 % sucrose (w/w), 50 mMTris-HCl pH 7.5, 5 mM EDTA), then the cells are homogenized with Ultra-turrax T8 (IKA Labortechnik) for 30 seconds cooled in ice-water and afterwards are centrifugated for 20 minutes at 14000 rpm at 4° C. The supernatant is discarded and the pellet is resuspended in 1 ml of TE buffer (50mM Tris-HCl pH 7.5, 1 mM EDTA) and the membranes are homogenized again by 10 strokes with pestle B (tight fitting) using ice cold Douce glass-glass homogenizer. 500 µl of membranes are aliquoted in each tube and are stored at - 80° C.

2.12 Radioligand binding assay

Receptor expression densities and binding affinities of different ligands in QBI-HEK293 cell line transiently expressing the 5-HT$_7$ receptor splice variants are determined by radioligandi binding assays.

Binding assays are performed in 96 well, round bottom microtiter plates with a total reaction volume of 100 µl, by performing saturation binding assay, receptor expression densities (B$_{max}$) and affinities of different ligands (K$_d$) can be estimated in the same assay. Scatchard analysis is performed with 5-HT$_{7(a)}$ receptor ligands [^{3}H]5-CT (5-Carboxamidotryptamine) and [^{3}H]SB269970 in the presence (non specific binding) or absence (total binding) of excess 5-HT. Specific binding is defined as the difference between total binding and non-specific binding.

G-protein coupled receptor may exist in different conformations, such as low and high affinity states. In the presence of GTP most receptors will exist in the low affinity state. GTP is included to avoid bias due to unpredictable ratios between the two affinity states.

An assay mix is performed with 100 µM of GTP and binding buffer 10X (500 mM Tris-HCl pH 7.5, 10mM EDTA, 50mM EGTA, 20mM MgCl$_2$, 10mM ascorbic acid, 1 % BSA) in dH$_2$O, 30 µl of this mixture is added to each well. Each radioligand stock solution is diluted 1:2 and are made 8 serial dilutions and 20 µl of each radioligandi dilution are added to one row of wells. This is repeated for each dilution, starting with
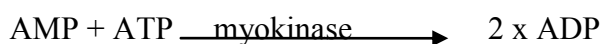
the lowest concentration in the top row of the 96-well plate. For the determination of accurate concentration of the radioligands, are prepared for each dilution 5 scintillation vials (Polyethylene vials, Packard BioScience) containing 20 µl of radioligand and 3 ml of scintillation fluid (Ultima Gold XR, Packard), the samples are counted in the Wallac Winspectral^{TM} 1414 Liquid scintillation Counter, Perkin Elmer. 30 µl of cold 5-HT and 30 µl of H_2O are added to each well to determine total and non-specific binding. The 20 µl of membrane preparation are added to each well and the plate is mixed by vortexing and incubated at room temperature for 1 hour. Afterwards the membranes are harvested onto Whatmann GF-2 filter (Packard) pre-soaked in 0.3 % of polyethylenemine, with a Packard Cell Harvester (Packard). The membranes are washed 4-6 times with cold washing buffer (50 mMTris-HCl pH 7.0, 2 mM $MgCl_2$). The filters are dried at 37° C for 45 minutes and then 20 µl of MicroScint scintillation fluid (Packard) are added to each well. The filter plates are counted later in a Packard TopCount Scintillation Counter (Packard).

2.13 Adenylyl cyclase assay

The adenylyl cyclase activity is measured by determining conversion of [α-^{32}P]ATP to [^{32}P]cAMP in membrane preparations. G_s-coupled receptors regulate adenylyl cyclase activity, stimulating this enzyme. Agonist-bound receptors catalyse the release of GDP bound to the α-subunits of the heterotrimeric membrane-bound G proteins. This is followed by GTP binding and the G protein dissociation into a βγ subunit and an active α-subunit (G_α). There are two classes of α-subunit, $G_{\alpha s}$ and $G_{\alpha i}$, which regulate adenylyl cyclase activity. $G_{\alpha s}$ stimulates and $G_{\alpha i}$ inhibits adenylyl cyclase.

Adenylyl cyclase activity is measured in a final volume of 50 µl, containing 10 µl of crude membrane preparations, 20 µl of additives and 20 µl of an assay mix composed of: Incubation mixture (IM) solution (Tris-HCl, EDTA, cAMP and [^{3}H]cAMP), ATP, [^{32}P]ATP, GTP, $MgCl_2$, ATP-regenerating system (RS solution), IBMX solution (3-isobutyl-1-methylxantine) and dH_2O. ATP is in the concentration range 0.1 mM with specific activity at about 200 cpm/pmol (calculated for each assay). EDTA is included to permit linear cAMP accumulation over extended periods of time. GTP is added as substrate for activation of the G protein to obtain hormonal stimulation

of adenylyl cyclase. The main substrate for the enzyme is Mg-ATP rather than ATP, so an excess of Mg^{2+} (4 mM) over EDTA and ATP is needed to obtain enzyme activity. Terminal phosphatases, such as ATPases, present in the membrane preparation may alter the level of substrate available for the enzyme. This is prevented by an AP-regenerating system (RS) containing myokinase (40 U/ml), creatin phosphokinase (0.2 mg/ml) and creatinephosphotase (20 mM).

$$AMP + ATP \xrightarrow{\quad myokinase \quad} 2 \times ADP$$

$$Creatin\text{-}PO_4 + ADP \xrightarrow{\quad creatin\ phosphokinase \quad} ATP + creatine$$

Membrane preparations also contain phosphodiesterase activity. To prevent breakdown of the generated $[^{32}P]cAMP$ formed and $[^3H]cAMP$, the phosphodiesterase inhibitor IBMX (1 mM) together with unlabeled cAMP (1mM) is included in the assay mix. The reaction products are separated by sequential chromatography on Dowex 50 cation exchanger and on neutral aluminium oxide (Alumina) columns as originally described by Salomon et al. with minor modifications. The recoveries of each sample through the columns are monitored by adding $[^3H]cAMP$ (10000 cpm/reaction) to assay mix, thus eliminating individual difference between the columns.

In a tube kept on ice the following reagents are mixed together to prepare the assay mix as below:

Content	Stock concentration	Final concentration (50 μl)	Volume per reaction (μl)
IM (Incubation Mix)	10 X (205 mM Tris-HCl pH 7.6, 10 mM cAMP, 10 mM EDTA, $[^3H]$-cAMP ~2000 cpm/μl)	1 X	5.0 μl
RS (Regenerating System)	10 X (200 mM creatinephosphatise, 2 mg/ml creatine phosphokinase, 400 U/ml myokinase)	1 X	5.0 μl
GTP	10 mM	20 μM	0.1 μl
MgCl$_2$	100 mM	4 mM	2.0 μl
IBMX	25 mM	1 mM	2.0 μl
ATP/[α-^{32}P]ATP	100 mM	0.1 mM	5.0 μl
dH2O	(10^6cpm/5 μl)		0.9 μl
total			20 μl

The additives are prepared and diluted in 0.1% BSA/1 mM ascorbic acid respectively to the final concentration: Forskolin 100 µM, 5-HT 100 µM, 5-CT 10 µM, SB269970 100 µM. For concentration-response curve of 5-HT, 5-CT and SB269970, a serial 1:2 dilution of the final concentration (5-HT 100 µM, 5-CT 10 µM, SB269970 100 µM) is performed to achieve 21 different concentrations. The stock Forskolin solution is diluted to obtain the final concentration (100 µM) and to achieve 3 tubes for each sample with the same concentration. The reaction tubes are kept on ice and 20 µl of each additives dilutions are added. Other 20 µl of 0.1% BSA/1 mM ascorbic acid are used to perform 3 tubes for basal and blank samples respectively.

Afterwards a vial of membrane preparation is thawed on ice and 10 µl are used in each reaction tube, 10 µl of TE buffer are added to the blanks tubes. 20 µl of assay mix prepared before are added to each tube, the reaction tubes are mixed by vortexing and transferred to a shaker water bath at 32° C and incubated for 20 minutes, then 100 µl of STOP solution (10mMcAMP, 40mM ATP, 1% SDS) are added to each reaction tube.

The chromatography separation starts with the equilibration of the Dowex 50 columns with ~ 10 ml of dH_2O, the columns should drain completely before use. 850 µl of dH_2O are added to each reaction tube and are poured in to Dowex columns and to wait that the columns are completely drained. The Dowex columns containing the samples are washed with 2 + 2 ml of dH_2O, respectively. The rack of Dowex columns are placed on the top of the Alumina columns (pre-equilibrated before with ~10 ml of imidazole-HCl buffer), the reaction products elute from dowex columns into Alumina columns with 4 ml of dH_2O. The Alumina columns containing the samples are washed with 2 ml of imidazole-HCl buffer. The rack of Alumina columns are placed now on the top of a rack of counting vials, filled with 3.5 ml scintillation fluid (Ultima Gold XR, Packard); 3.5 ml of imidazole-HCl buffer are added to the Alumina columns and the reaction products are eluted to the counting vials. The vials are capped and shaked well and counted in the Wallac Winspectral™ 1414 Liquid scintillation Counter, Perkin Elmer. After use the Dowex columns are regenerated by sequential washing with ~ 10 ml of each of 2 M NaOH, dH_2O, 2 M HCl and 2 x dH_2O, then the columns can be stored dry and need only to be reequilibrated with dH_2O before use. The Alumina columns are washed with ~ 10 ml of dH_2O and stored in water after use, these columns have to be reequilibrated with 10 ml imidazole-HCl buffer before use.

2.14 Protein quantification

The amount of protein in membrane preparation is determined by using the microBC Assay protein quantification kit (Uptima). This assay is a colorimetric assay based on the Biuret reaction. In an alkaline solution peptidic bonds of protein reduces Cu^{2+} to Cu^+. Two molecules of bicinchoninic acid (BCA) chelates Cu^+ ion with very high specificity and forms a water soluble purple colored complex which has an absorption maximum at 562 nm. The absorbance is directly proportional to the initial protein concentration between 1-20 µg/ml, allowing for spectrophotometrical quantification of protein content in an aqueous solution.

Triplicates of BSA standards samples are prepared with the following concentration: 0, 1, 2.5, 5, 7.5, 10, 15, 20 µg protein in a 96-well plate; dH_2O is used as zero standard. From the binding assay are used 20 µl of membrane preparation samples and 10 µl from the adenylyl cyclase assay that are pipetted in 5 different wells. 30 µl of dH_2O are added to the standards and 50 µl to the samples. 10 µl of 1 % of SDS are added to each well of the plate. The MicroBCassay working reagent is prepared as a mixture between the solutions A+B+C in the ratio 25:25:1 and 80 µl of this mixture are added to each well. The plate is covered with plastic tape and mixed gently on a plate shaker for 30 seconds, then it is incubated at 60° C for 1 hour. The absorbance is measured at 570 nm in a Perkin Elmer HTS 7000 Bio Assay Reader. Standards curve are prepared by plotting absorbance of the standard versus the amount of protein and to quantify the amount of protein in the samples from linear parts of the curve.

2.15 Calculations

Binding and adenylyl cyclase data are analyzed by non-linear regression using Microsoft Excel 2007 with the Solver add-inn, using the following equations.

*Saturation binding.*The non-specific binding was assumed to be linear and analyzed by linear regression. The concentration of free [³H]5-CT was estimated as the difference between [³H]5-CT added and [³H]5-CT bound (non-specific or total), and

this estimate was used in all further calculations. The specific binding data were fit to the equation:

$Y = B_{max}x/(K_d+x)$

where B_{max} is the total number of specific binding sites (receptors), K_d is the equilibrium dissociation constant and x is the concentration of free [^{3}H]5-CT.

Competitive binding assays. The data were fit to the equation:

$Y=a+(b-a)/(1+x/c)$

where a is non-specific binding, b is total binding in the absence of competitor, c is IC_{50}, and x is the concentration of competitor.

Activation of adenylyl cyclase. The data were fit to the equation:

$Y=a+(b-a)x/(c+x)$

where a is basal adenylyl cyclase activity, b is maximal adenylyl cyclase activity stimulated by the agonist, c is EC_{50}, and x is the concentration of agonist.

Antagonism of 5-HT-evoked adenylyl cyclase stimulation. The data were fit to the equation:

$Y=b+(a-b)/(1+x/c)$

where a is agonist-stimulated adenylyl cyclase activity in the absence of antagonist, b is agonist-stimulated adenylyl cyclase activity in the presence of a saturation concentration of antagonist, c is IC_{50}, and x is the concentration of antagonist.

2.16 SDS-PAGE and Western blotting analysis

The separation of macromolecules in an electric field is called *electrophoresis*. A very common method for separating proteins by electrophoresis uses a discontinuous polyacrylamide gel as a support medium and sodium dodecyl sulfate (SDS) to denature the proteins. The method is called sodium dodecyl sulfate polyacrylamide gel electrophoresis (SDS-PAGE). SDS (also called lauryl sulfate) is an anionic detergent, meaning that when dissolved its molecules have a net negative charge within a wide pH range. A polypeptide chain binds amounts of SDS in proportion to its relative molecular mass. The negative charges on SDS destroy most of the complex structure of proteins, and are strongly attracted toward an anode (positively-charged electrode) in an electric field. Protein separation by SDS-PAGE can be used to estimate relative molecular mass,

to determine the relative abundance of major proteins in a sample, and to determine the distribution of proteins among fractions.

2.16.1 Sample preparation

The membrane preparations are properly thawed and the samples are diluted to desired concentration using TE buffer. To each sample ¼ of total sample volume of 4X SDS-gel loading buffer activated with 10 % of β-mercaptoethanol is added. All samples are kept on ice before to load them on the gel.

2.16.2 Gel casting

Many systems for protein electrophoresis have been developed, and apparatus used for SDS-PAGE varies widely. A Mini-PROTEAN Tetra Electrophoresis System (Bio-Rad) is used. Gels are usually polymerized between two glass plates in a gel caster. The glass plates, one long with attached spacers and one short for each gel, are washed three times with dH_2O and 75% EtOH. The glasses are put into holder, ensure bottom edges of the two plates are well aligned and cleaned with air to remove any fibres and clipped into stand. 10 ml of 8 % SDS-acrylamide separating gel solution is prepared (dH_2O, 30% acrylamide mix (acrylamide/bis N,N'-methylene-bis-acrylamide), 1.5 M Tris-HCl pH 8.8, 10 % SDS, 10 % APS, TEMED (not add APS and TEMED until ready to cast). About 4-5 ml of separating gel are poured between the assembled glass plates and sufficient place is left for the stacking gel. Carefully overlay the acrylamide solution with 150-200 μl of n-butanol to ensure a flat surface. Leave the gel solution to set for about 30 minutes at room temperature. Afterwards the n-butanol solution is washed away with water and removed remaining water with filter paper. A5% polyacrylamide stacking gel solution is prepared (dH_2O, 30% acrylamide mix (acrylamide/bis N,N'-methylene-bis-acrylamide), 1.0 M Tris-HCl pH 6.8, 10 % SDS, 10 % APS, TEMED) and poured on top of separation gel. The specific comb is put in place and let the stacking gel polymerize for approximately 20-30 minutes at room temperature.

2.16.3 Gel running

While the stacking gel is polymerizing, prepare the samples by heating them to 95-100° C for 3-5 minutes in 1X SDS- gel loading buffer to denature the proteins. After polymerization is completed, the Teflon comb is removed carefully and washed with 1X Tris-glycine electrophoresis running buffer. The gel is mounted in the electrophoresis apparatus and the tank is filled and inner chamber with 1X Tris-glycine electrophoresis buffer. 15 µl of each preheated sample and 7µl of specific molecular weight standards (Precision Plus Protein Dual Color Standards, Bio-Rad) are loaded into the gel. The electrophoresis apparatus is attached to a power supply (BioRad Power Pack 300). The protein samples run through the stacking gel at constant current (A) of 20 mA, when the dye front has reached the resolving gel the current is increased to 45 mA. The gel should run until the dye front reaches the bottom of the resolving gel.

2.16.4 Western blotting

The 1X transfer buffer is prepared from the stock solution 10X (313 mMTris base, 2.4 M glycine), methanol and dH_2O is added until 700 ml. The transfer buffer is poured into a tank and are added (per gel) 6 pieces of filter paper, 2 pads and an activated (15 seconds pre-treatment in methanol) PVDF (polyvinylidenedifluoride) membrane. The tank is put in freezer for 1 hour. When gel separation is finished the glass plates are removed, the stacking gel and any residual gel around the edge are separated and removed. The pads are placed onto blotting mesh folder and covered with 2 pieces of filter paper. The 3[rd]piece of filter paper is put onto the gel, turned over and the gel is removed from glass (using spatula) and then is put onto the other filters paper. The gel is covered with the PVDF membrane (smoothen away bubbles) and then it is covered with 3 pieces of filter paper and another pad. The mesh folder is closed and put into the blotting tank. The membrane must be closest to the red (+) pole and the gel closest to black (-) pole. A magnetic stirrer and an ice block are added to cool the system under blotting process. For transferring a current of 400 mA is used to pull the protein from the gel into the PVDF membrane.

2.16.5 Immunodetection

After transferring the membrane is incubated on a shaker for the non-specific block for 1 hour in 10 ml of 5% non-fat dry milk in phosphate buffered saline (PBS)/Tween 20 (0.05 %) at room temperature, afterwards a primary antibody (rabbit, Oncogene) is diluted to the desired concentration in 5% milk-PBS/Tween 20solution and the membrane is incubated with the primary antibody solution over night at 4° C. The next day the membrane is washed 3 times, each one for 5 minutes with PBS/Tween 20, then a secondary antibody (ECL^{TM} Anti-rabbit IgG Horseradish Peroxidase Linked) is diluted to the desired concentration in 5 % milk-PBS/Tween 20 solution and the membrane is incubated in this solution for 1 hour at room temperature. Afterwards other 3 washes for 5 minutes in PBS/Tween 20 are repeated at room temperature and then the membrane is rinsed with dH$_2$O to remove Tween 20 until it is free from foam and prepared to the detection by chemiluminescense (LumiGLO Solution). The membrane is put into a container with pre-prepared detection substrate (chemiluminescence reagent containing HRP substrate) and incubated on a shaker at room temperature for 1 minutes. Afterwards the membrane is placed between two clean acetate sheets for scanning and exposed for appropriate time using UCP Sensicam (UVP Inc., CA, USA).

2.17 Molecular Dynamics

Molecular Dynamics (MD) is a form of computer simulation where atoms and molecules are allowed to interact with each other according to the laws of physics. Being the molecular systems made by a large number of particles, it is impossible to do an analytical analysis of the system properties. MD avoids this problem by means of numerical methods. One of the most significant advantages in MD is the consideration that molecules are *machines in motion*, thus MD investigates the relationship between structure, movement and function of macromolecules.

In chemistry and biophysics, the interaction between particles is either described by a "force field" (classical MD), a quantum chemical model, or a mix between them.

These terms are not used by physics, where interaction between particles are described by "potential functions".

In chemistry, MD is used as an important tool in protein structure determination and refinement of X-ray crystallography and NMR structures. MD has also been applied as a method of refining protein structure prediction. In fact protein folding is influenced not only by primary structure of protein but also by other factors as: proteins chaperone, metal factor, cell environment, concentration gradients, potential gradient.

A molecular dynamics simulation should take account for the available computational resources. Simulation size (n=number of particles), time-step and total time duration must be selected so that the calculation can finish within a reasonable time period. However, the simulations should be long enough to be relevant to the time scales of the processes studied.

To make statistically valid conclusions from the simulations, the time span simulated should match the kinetics of the natural process. To obtain these simulations, several CPU-days to CPU-years are needed. Parallel algorithms allow the load to be distributed among CPUs.

During a classical MD simulation, the most CPU intensive task is the evaluation of the potential (force field) as a function of the particles internal coordinates. Within that energy evaluation, the most expensive one is the non-bonded or non-covalent part. Another factor that impacts total CPU time required by a simulation is the size of the integration timestep. This is the time length between two recurrent evaluations of the potential. Typical timesteps for classical MD are in the order of 1 femtosecond (1E-15 s). This value may be extended by using algorithms such as SHAKE, which fix the vibrations of the fastest atoms (e.g. hydrogens) into place.

For simulating molecules in a solvent, a choice should be made between explicit solvent and implicit solvent. Explicit solvent particles (such as the TIP3P, SPC/E and SPC-f water models) must be calculated expensively by the force field, while implicit solvents use a mean-field approach. Using an explicit solvent is computationally expensive, requiring inclusion of roughly ten times more particles in the simulation. But the granularity and viscosity of explicit solvent is essential to reproduce certain properties of the solute molecules. This is especially important to reproduce kinetics.

In all kinds of molecular dynamics simulations, the box size must be large enough to avoid boundary condition artifacts. Boundary conditions are often treated by

choosing fixed values at the edges (which may cause artifacts), or by employing periodic boundary conditions in which one side of the simulation loops back to the opposite side, simulating a bulk phase.

Molecular dynamics simulation calculate temporal evolution of a molecular system by numerically integrating the system's classical equation of motion (Newton equation).

$$m_i \frac{\partial^2 r_i}{\partial t_i^2} = F_i = -\nabla_i V(r_1, r_2, ..., r_n) \; i=1,N \qquad (1)$$

The above N coupled equation are simultaneously solved to obtain the atomic positions and velocities as a function of time. Here m_i and r_i are the mass and position of particle i and $V(r_1, r_2, ..., r_n)$ is the potential energy function, that depends on the position of all N particles. The negative gradient of the potential energy function in comparison with the position of particle i is the force F_i acting on that particle.

To solve this set of coupled differential equations it is necessary to define the initial condition from which the integration starts. Those conditions include: initial position of all atoms and their velocities. For protein simulations the initial positions are given as .pdb files, which are converted for the software used in the MD simulation (for instance psf and .gro files for the NAMD and the GROMACS softwares respectively).

The starting velocities are assigned from a Maxwell-Boltzmann distribution at some relatively low temperatures in each of the three velocity components x, y, and z. The system is then slowly heated up to the desired simulation temperature.

The temperature at any given moment is defined in terms of the mean kinetic energy:

$$T(t) = \frac{1}{k_b M} \sum_{i=1}^{M} m_i |v_i|^2 \qquad (2)$$

M is the total number of unconstrained degree of freedom, v_i is the velocity of the particle i at time t, and k_b is the Boltzmann constant.

Every molecular dynamics simulation is divided into several stages:

- Model generation: generation of the molecular model (creation of box, solvation of system, addition of ions)
- Preparation: minimization of the initial structure and heating up to simulation temperature

- Equilibration: this is an important stage in which long dynamics trajectories are made in order to obtain equilibration of the system and therefore reliable results

- Production run: actual dynamics simulation from which data is accumulated

- Analysis: converts data of simulation in important information

To obtain molecular trajectories and velocities the MD software relies on an integration algorithm (integrator). The algorithm uses the finite difference method: given coordinates and velocities values at time t, the values are calculated by the integrator at time $t + \Delta t$; Δt is named timestep.

The most used integration algorithm in biomolecular simulation is the Verlet integrator, which is based on two Tailor expansion of velocity, forward expansion ($t + \delta t$) and backward expansion ($t - \delta t$).When performing numerical calculations it is important to be able to assess the quality of the procedure (its stability). Since Newton equation conserves energy (microcanonic system) a good simulation is expected to maintain the total energy fixed. One measure for its stability is the ratio between the average fluctuation of total energy $<\Delta E> = <E(t)-<E>>$ and the average total energy of the system $<E>$: $<\Delta E>/<E>$. This ratio must be smaller than 10^{-3} to consider the simulation stable.

During MD simulation the temperature must be controlled. As defined above the temperature is related to the kinetic energy of the system, therefore the MD simulation is dramatically affected by the temperature.

2.17.1 Forcefield

The complete representation of a molecule need the resolution of the Schrödinger equation (4):

$$H\Psi(r,R) = E\Psi(r,R) \quad (4)$$

This equation cannot be solved without approximation for systems that are not hydrogenoid atoms. With the introduction of the Born-Oppenheimer approximation the equation (4) could be divided in two equations:

$$H\psi(r,R) = E\psi(r,R) \quad (5)$$

$$H\Phi(R) = E\Phi(R) \quad (6)$$

Equation (5) describes motion of electrons and equation (6) describes motion of atoms. The basis of this approximation is that the motion of electrons is faster respect to the motion of atoms. Calculation of trajectories by equation (6) needs the potential energy obtained by the solved equation (5). To overcome complicated quantomechanic calculations on equations (5), others approximation can be used:

- Empirical potential energy
- Substitution of equation (6) with Newton equation (7), since atoms are more heavy than electrons and thus quantomechanic effects are negligible.

$$-\frac{\partial V}{dR} = m\frac{\partial^2 R}{d\hat{t}} \quad (7)$$

The potential energy describes all intra- and intermolecular interactions, thus the choice of a potential energy function (forcefield) has severe influence on the reliability of MD calculations.

The construction of a forcefield relies on the combination of coordinates, bond parameters (distance, angles) and non-bonds parameters (electrostatics, Van der Waals radii).

The forcefield indirectly relies on quantistic effects, due to its modeling on real molecules.

Forcefields used in MD do not describe chemical events as acid-base reactions, photochemical reactions, electron transfer events.

The forcefield is a sum of parameters, each describing different nuclear interactions in a molecule.

A forcefield is more accurate if it is specific for a particular molecular system. Forcefield parameters are obtained from *ab initio* calculation: energy, gradient of energy and Hessian are calculated for low and high energy conformations of sample molecules. Forcefields are useful tools for the study of system where quantistic effects are not effective as macromolecules, crystal morphology and organic-inorganic interphases.

2.18 Molecular docking

In the field of molecular modeling, docking is a method which predicts the preferred orientation of one molecule to a second when bound to each other to form a stable complex. Knowledge of the preferred orientation in turn may be used to predict the strength of association or binding affinity between two molecules using for example scoring functions.

Molecular docking can be thought as a problem of *"lock-and-key"*, where one is interested in finding the correct relative orientation of the *"key"* which will open up the *"lock"* (where on the surface of the lock is the key hole, which direction to turn the key after it is inserted, etc.). Here, the protein can be thought as the "lock" and the ligand can be thought of as a "key". Molecular docking may be defined as an optimization problem, which would describe the "best-fit" orientation of a ligand that binds to a particular protein of interest.

3 RESULTS

3.1 Preliminary structural model of 5-HT$_{7(a)}$ receptor

The homology model of the human 5-HT$_{7(a)}$ receptor was built basing on the 2.4 Å resolution crystal structure of the β$_2$ adrenergic-receptor (pdb entry: 2rh1) as a template. This is a structure of the β$_2$ receptor in complex with the antagonist/inverse agonist carazol (therefore represents an inactive state conformation of the receptor). The model has been renumbered according to the SwissProt sequence of the human 5-HT$_7$ receptor. Conformation of residues that differ between the 5-HT$_7$ and β$_2$ receptors have been slightly optimized using the refineModel macro of ICM. In accordance with the template structure, the homology model features a disulfide bridge between TMH3 and extracellular loop 2. The same is for the 5-HT$_{1a}$ model receptor.

Molecular dynamics simulations were carried out with the program NAMD 2.7, developed by *Theoretical and Computational Biophysics Group* to the*Beckman Institute for Advanced Science and Technology*- University of Illinois at Urbana-Champaign.

CHARMM27 was the forcefield used for all-atom simulations.

TIP3P was used as the explicit water model with 1 as the dielectric constant (ε). In explicit water models the dielectric constant is a property related to the collective polarizability of the environment.

The parameter file .prm used for the modeling of molecular interactions is par_all27_prot_lipid.prm. This parameter file contains all the numerical constants needed to evaluate forces and energies, given the forcefield and the PSF file of the system (protein in a membrane environment).

1-4 scaling factor value was 1. It means that 1-4 interactions were fully included.

Cut-off values for non-bonded interactions (Coulomb and Van der Waals forces) was 10 Å.

Cut-off values for the switching function was 9Å.

Langevin dynamics was used for all thesimulations. The value of the friction coefficient γ was 1 ps^{-1}. Langevin dynamics mimics the viscous aspect of the solvent. The Langevin equation is a *stochastic* differential equation in which two force terms have been added to Newton's second law to approximate the effects of neglected

degrees of freedom. One term represents a frictional force –yidr$_i$/dt, the other a *random force* R$_i$.

$$m_i \frac{d^2 r_i}{dt^2} = -\gamma_i \frac{dr_i}{dt} + F_i + R_i$$

The SHAKE algorithm was used to fix the length of covalent hydrogen bonds, in order to use a timestep of 2 fs.

Non-bonded interactions were calculated every step.

The protocol of simulations (NPT)is below reported:

1. Cubic box: Bilayer of POPC (palmitoyl-oleil-phosphatidylcoline); patch dimensions 100x100 Å
2. Settled temperature: 300 K
3. Settled pressure: 1 atm
4. Insertion of the membrane protein into the bilayer, hydration
5. Elimination of superimposed molecules of POPC and water and neutralization of the box (conc. Salt 0.150 mM)
6. Energy minimization of the protein
7. Equilibration of lipid tails: 500 ps
8. Equilibration of lipids and water: 500 ps
9. System Equilibration: 1ns (time step 1ft)
10. Moleculare Dynamics: 30 ns (time step 2ft)

Molecular Dynamics simulations were run on a PC-Linux Cluster.

Molecular Dynamics calculations were carried using computational resources granted from the supercomputing HPC-CASPUR and HPC-CINECA.5 ns of simulation require 96 h distributing the calculations on 16 processors.
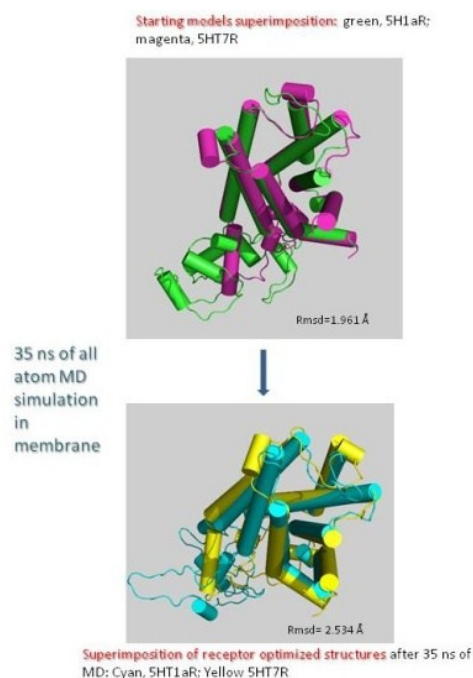
Fig.6: Overlapping of the starting homology models and the optimized structures of $5HT_{1A}$ and $5HT_7$ receptors.

Using the structural model of the 5-HT$_7$receptortwo important regions are pointed out: the 7[th]transmembrane helix (TMH7), involved in the binding activity, and the second intracellular loop (ICL2) involved in the activation process. In each region some amino acid residues are important for the receptor's activation and for its functional activity, then these residues are analyzed with site-directed mutagenesis.

The amino acid residues indentified and located in the 7[th]transmembrane helix are: Glu366, Arg367, Tyr374, Trp364, Trp371, Arg389 and Asp390. While the residues located in the second intracellular loop are : Thr185, Arg186, Tyr190, Arg193 and Lys197 (fig. 7).
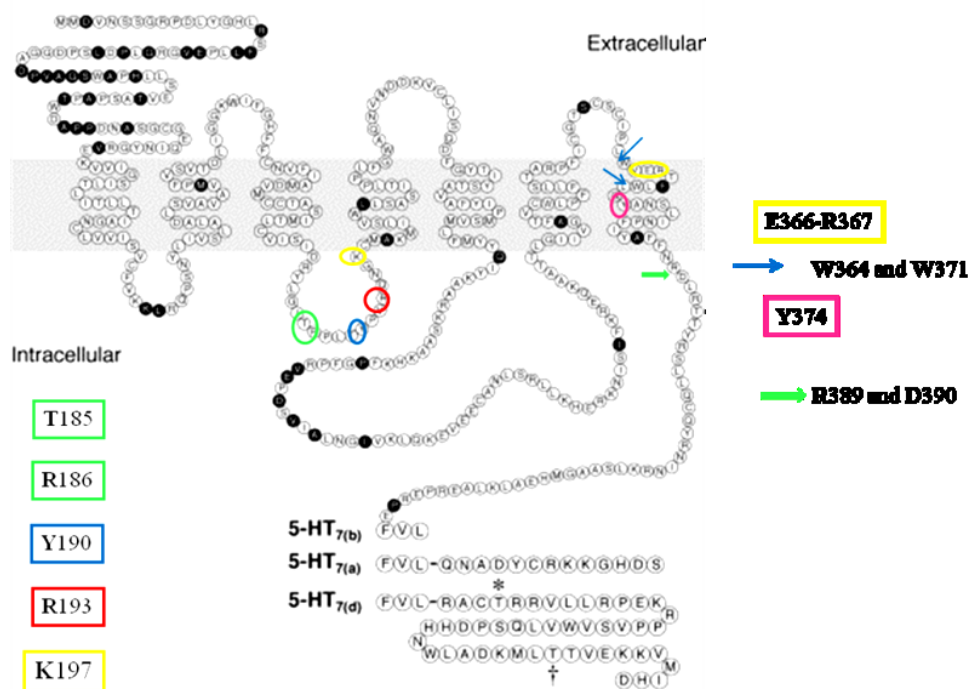
Fig.7: Localization of specific residues for the receptor's activation in the 7[th]transmembrane helix and in the second intracellular loop

3.2 Site-directed mutagenesis analysis

Mutations in the human $5\text{-HT}_{7(a)}$ receptor are carried out using the QuikChange® Site-Directed Mutagenesis kit (Stratagene) by a *Pfu*Turbo DNA polymerase and a thermal temperature cycler.

The amino acid residues on the 7[th]transmembrane helix are mutagenized as follow: **E366T**, **E366R**, **E366D**, **E366A**;**R367V**;**W364V**;**W371V**;**Y374A**, **Y374F**, **Y374T**;**R389D**and**D390K**. While the amino acid residues located in the second intracellular loop are mutated all of them in **Ala** (**T**185A, **R**186A, **Y**190A, **R**193A, **K**197A).

The desired mutation (single point) should be in the middle of the primer with ~ 10-15 bases of correct sequence on both sides.

The oligonucleotide primers Forward and Reverse, are extended during thermal cycling. The samples reactions are prepared as below:

- ✓ 5 µl of 10X reaction buffer
- ✓ 2.2 µl of dsDNA template (9 ng/µl)
- ✓ 1.5 µl of oligonucleotide primer Forward (100 ng/µl)
- ✓ 1.5 µl of oligonucleotide primer Reverse (100 ng/µl)
- ✓ 1 µl of dNTP mix
- ✓ ddH$_2$O to a final volume of 50 µl
- ✓ 1 µl of *Pfu Turbo* DNA polymerase (2.5U/µl)

Each cycle reaction using the cycling parameters outlined in table 3

Cycles	Temperature	Time
1	95° C	1'
18	95° C	50''
	60° C	1'
	68° C	8' 30''
1	68°C	7'

Table 3: Cycling parameters used for each cycle reaction

Afterwards follows an 0.8 % agarose gel electrophoresis in TAE 1X. To check the PCR product 10 µl of the reaction mix is loaded on the gel with 7 µl of DNA marker 1 kb plus ladder
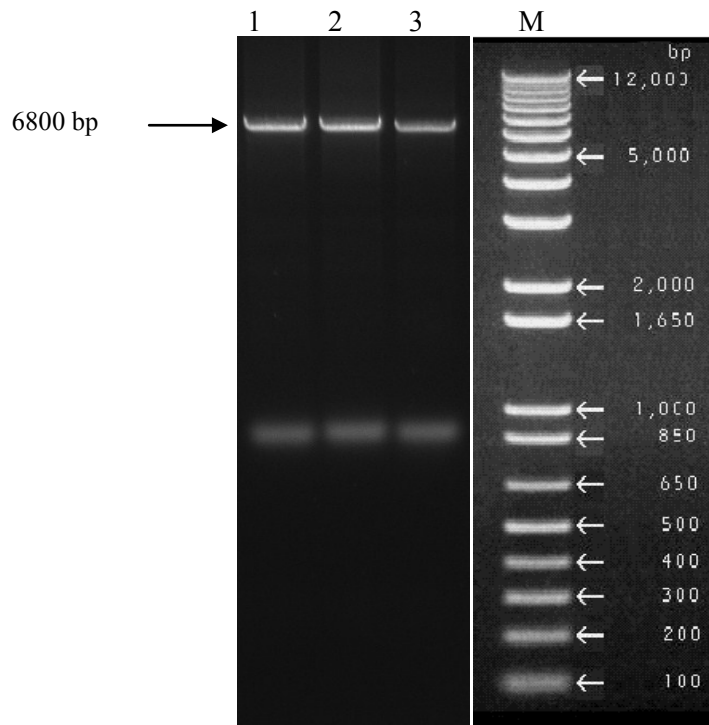
Fig. 8: Separation of mutated PCR product in 0.8 % agarose gel electrophoresis using as marker (M)1kb plus ladder (Gibco BRL) and in 1-2-3 wells the PCR mutated products (~ 6800 bp)

3.3 Mutated plasmid preparation

Two different procedures are used to prepare the mutated plasmid. The first one is the Wizard ® Plus SV Miniprep kit (Promega). 4 clones for each mutant are picked from specific transformation plates, grown in LB medium and incubated O.N. at 37° C in a horizontal shaker. The following day 4 ml of overnight bacterial culture are used to extract the mutated DNA for each mutant. At the end the quality of the mutated DNA is checked on 0.8 % agarose gel electrophoresis using 1 kb plus ladder as DNA marker.
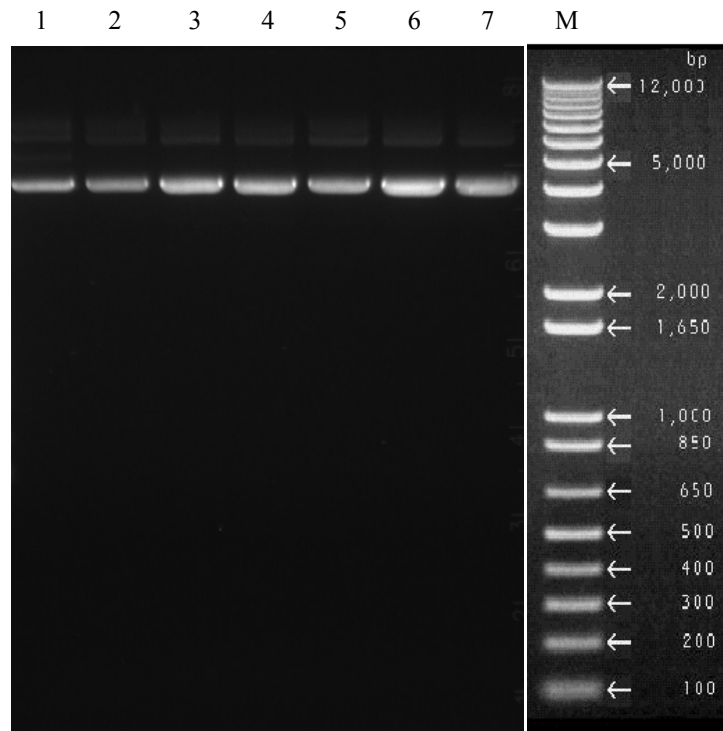
Fig. 9: DNA mutated preparation using the Miniprep kit from Promega, the 1 kb plus ladder standard marker is used and in the first well is loaded the cloning product (pcDNA3.1 plasmid and 5-HT$_{7(a)}$ gene coding), form well 2 to 7 some examples of mutated clones.

The mutated clones purified are used in sequencing procedure to check that the exact mutation in each mutant is inserted properly.

The second procedure to prepare the mutated DNA is performed to obtain a larger amount of purified mutated plasmids. The large-scale plasmid preparation is set up using the Qiagen Plasmid Maxi Kit (QIAGEN). The purified plasmid in this case are used to express them in human QBI-HEK293 cells, important cell line to study the GPCRs; to prepare the membrane containing the specific mutant and to perform the functional assays (binding and adenylyl cyclase activity).

3.4 Radioligand binding assay

Receptor expression densities and binding affinities of different ligands in QBI-HEK293 cell line transiently expressing the 5-HT$_{7(a)}$receptor are determined by radioligand binding assays.

Binding assays are performed in a microtiter plates with a total volume of 100 µl, by performing saturation binding assay, receptor expression densities (B$_{max}$) and affinities of different ligands (K$_d$) can be estimated in the same assay. For every mutant indentified in the TMH7(E366T, E366R, E366D, E366A; R367V; W364V; W371V; Y374A, Y374F, Y374T; R389D and D390K) and in the ICL2 (T185A, R186A, Y190A, R193A, K197A) the Scatchard analysis is performed with 5-HT$_{7(a)}$ receptor ligands [^{3}H]5-CT (5-Carboxamidotryptamine) and [^{3}H]SB269970 in the presence (non specific binding) or absence (total binding) of excess 5-HT (10 µM). Specific binding is defined as the difference between total binding and non-specific binding. Saturation binding was performed for each mutant with up to 3 nM of [^{3}H]5-CT and up to 2.5 nM of [^{3}H]SB269970.

In the TMH7 the most important residues that after the mutation have changed the functional activity of the 5-HT$_{7(a)}$ receptor are Glu366, Tyr374, Arg389. The others amino acid residues (Trp364, Trp371, Arg367 and Asp390) in the TMH7 after the mutation have reduced or have not changed the receptor's activity (table 4).

MUTANT	[³H]5-CT		[³H]SB269970	
	K_d (nM)	B_{max} (pmol/mg protein)	K_d (nM)	B_{max} (pmol/mg protein)
5-HT$_{7(a)}$	0,33 ± 0,04	2,02 ± 0,30	0,49 ± 0,11	1,78 ± 0,21
W364V	0,29 ± 0,08	1,94 ± 0,09	0,55 ± 0,17	1,92 ± 0,21
Y374A	0,44 ± 0,21	0,06 ± 0,02	0,77 ± 0,36	0,12 ± 0,04
E366T	N.D.	N.D.	N.D.	N.D.
E366R	N.D.	N.D.	N.D.	N.D.
E366D	0,69 ± 0,14	2,14 ± 1,01	0,32 ± 0,05	2,08 ± 0,63
E366A	0,89 ± 0,78	0,82 ± 0,35	0,98 ± 0,60	1,39 ± 0,13
R367V	1,07 ± 0,85	0,17 ± 0,11	0,17 ± 0,01	0,26 ± 0,06
R389D	0,68 ± 0,06	0,53 ± 0,06	0,80 ± 0,004	0,46 ± 0,07
D390K	0,51 ± 0,08	1,22 ± 0,15	0,57 ± 0,11	1,09 ± 0,04

Table 4: Total receptor levels (B_{max}) and binding affinities (K_d) determined by radioligand binding assays with increasing concentration up to 3 nM of [³H]5-CT and 2.5 nM of [³H]SB269970 in absence (total) and presence (non-specific) of 10 μM 5-HT for 1 hour at 24° C obtained from the respectively membranes. Data are mean ± S.E.M. from 3-5 experiments

The residue Glu366 at the beginning was mutated in Thr (E366T) to remove the negative charge in this part of the receptor and this new receptor showed a complete lack of ability to bind any of the ligands. To understand which kind of interaction there is in this part of the receptor between the ligands and the receptor, other mutations were performed on the E366: to Asp (E366D) to understand the importance of amino acid charge; to Ala (E366A) to test if the length of the side chain is important to bind the ligands and to Arg (E366R) to see if there are some electrostatic interactions involved. These new mutants (E366D, E366A, E366R) were analyzed in the same conditions in the binding assays as before and as predicted the most important result was obtained by the mutation E366R, in this case the receptor has again lost the ability to bind the ligands, while the receptor E366A has reduced the ability to bind the specific ligands.

A mutation in the neighboring residue, R367V, resulted in a decreased ability to bind the ligands (both agonist and antagonist) but it didn't change the ability to activate the G-protein and then the adenylyl cyclase. Similar results were obtained with the

mutant R389D where the positive charge was replaced by a negative one, while the mutation D390K and the double mutant R389D-D390K didn't change the receptor's activity.
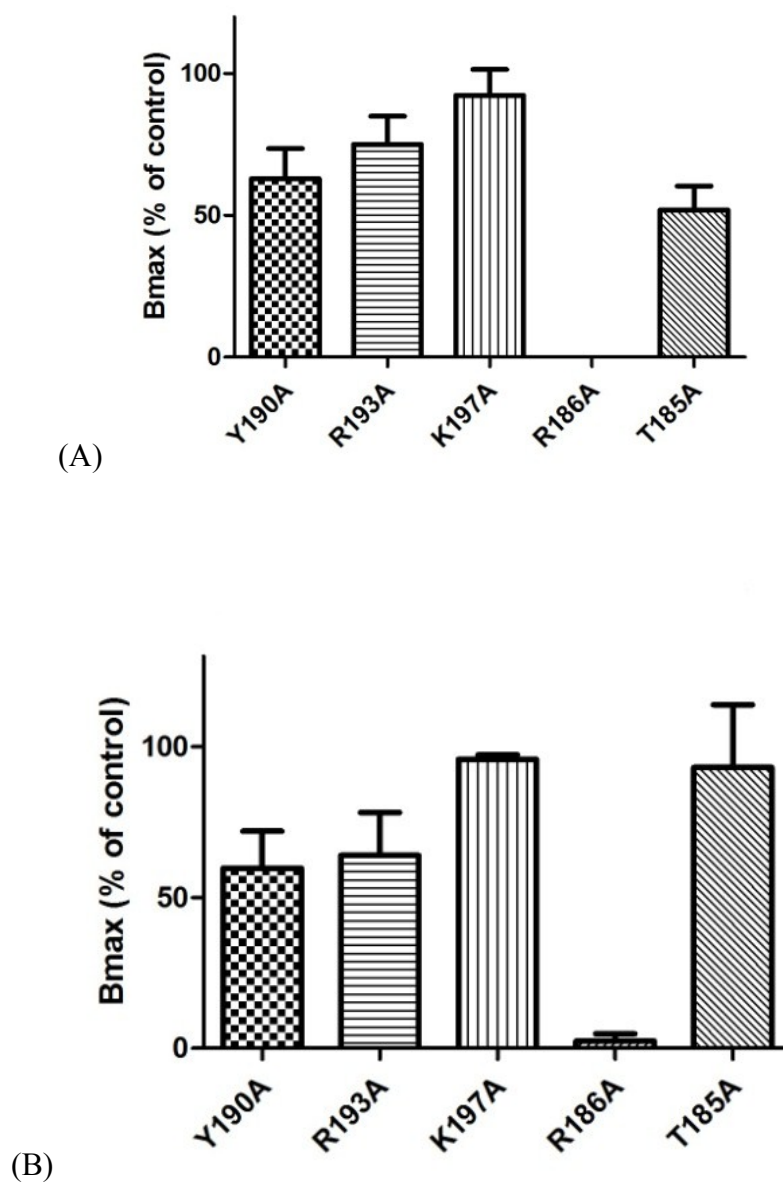

(A)

(B)
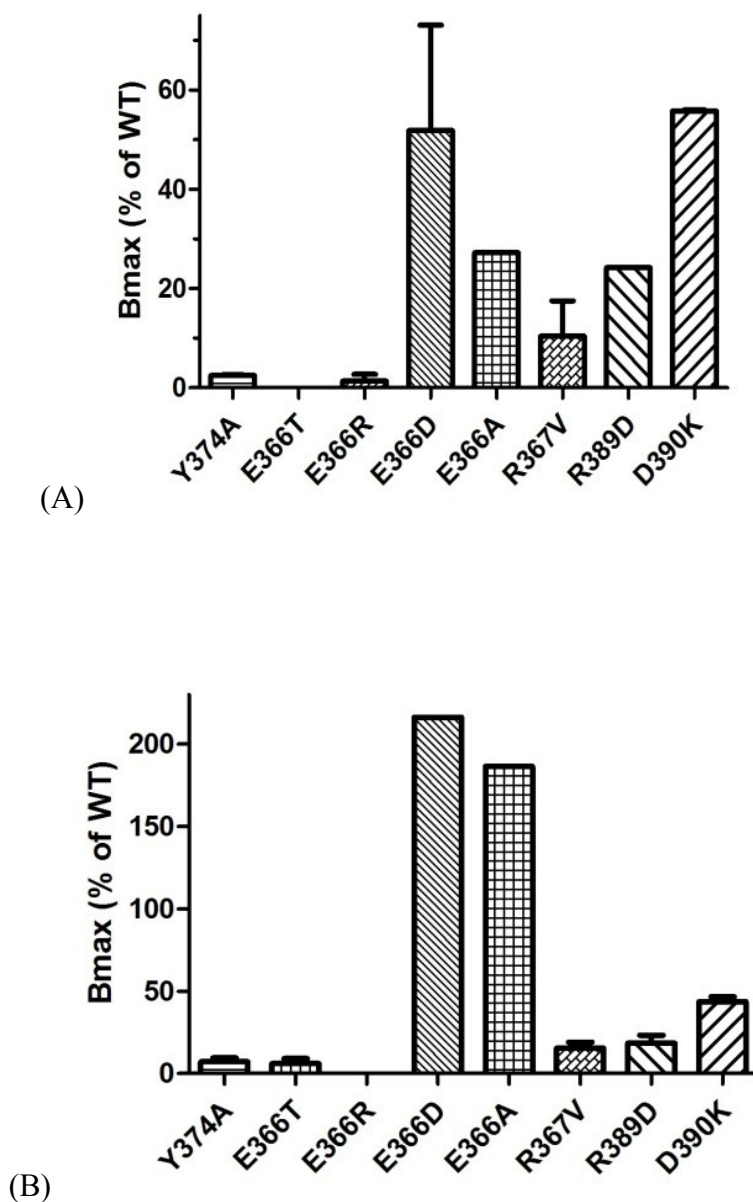
Fig.10: Receptor densities (B_{max}) of the most important mutants in the TMH7. (A) B_{max} of mutant receptors in membrane of QBI-HEK293 cells determined by [^{3}H]5-CT binding. (B) B_{max} of mutant receptors in membrane of QBI-HEK293 cells determined by [^{3}H]SB269970 binding. Data are presented as receptor densities as percent of their respective controls (sister plates transfected with the wild-type 5-HT$_{7(a)}$ receptor)

Another important mutant receptor in the TMH7 was Y374A, this was created removing the aromatic group from the residue Tyr374. The mutation caused a differential change in affinity between agonist and antagonist ligands. Furthermore the binding affinity of both ligands was reduced with some more effect on the antagonist than agonist affinity. To understand why there are these differences between the two different kind of ligands and to point out which part of this residue (aromatic group or OH-group) is involved in the binding process other mutants were created on the Tyr374. The new receptors are Y374F (to see if in this part of the receptor the OH-group is important) and Y374T (to understand if the phenolic group is involved in the interactions with the ligands). The mutant Y374T showed a reduction in the ability to bind the ligands and once again a differential change in the affinity between the ligands is pointed out, while the mutant Y374F didn't change the ability to bind the agonist and antagonist ligands. These results indicate that the presence of the phenolic group is very important to establish some interactions with the specific ligands.

In the second intracellular loop (ICL2) all residues are mutated in Ala, (T185A, R186A, Y190A, R193A, K197A). After the mutation the most important residue that seem to regulate the receptor's binding process is Arg186 as showed in the table 5.

MUTANT	[³H]5-CT		[³H]SB269970	
	K_d (nM)	B_{max} (pmol/mg protein)	K_d (nM)	B_{max} (pmol/mg protein)
5-HT$_{7(a)}$	$0,54 \pm 0,15$	$2,47 \pm 0,57$	$0,50 \pm 0,09$	$2,98 \pm 0,81$
Y190A	$0,25 \pm 0,06$	$1,50 \pm 0,33$	$0,38 \pm 0,07$	$1,86 \pm 0,12$
R193A	$0,27 \pm 0,04$	$1,64 \pm 0,53$	$0,45 \pm 0,11$	$1,79 \pm 0,56$
K197A	$0,58 \pm 0,14$	$3,13 \pm 2,15$	$0,76 \pm 0,20$	$3,17 \pm 1,86$
R186A	N.D.	N.D.	N.D.	N.D.
T185A	$0,70 \pm 0,30$	$0,89 \pm 0,17$	$0,83 \pm 0,21$	$1,50 \pm 0,30$

Table 5: Total receptor levels (B_{max}) and binding affinities (K_d) determined by radioligand binding assays with increasing concentration up to 3 nM of [³H]5-CT and 2.5 nM of [³H]SB269970 in absence (total) and presence (non-specific) of 10 μM 5-HT for 1 hour at 24° C obtained from the respectively membranes. Data are mean ± S.E.M. from 3-5 experiments

The residue Arg186 was mutated in Ala and after this mutation the receptor showed a complete loss of binding of both agonist and antagonist ligands.

The others mutants created in the ICL2 didn't change the receptor's binding process.

(A)

(B)

Fig.11: Receptor densities (B_{max}) of the most important mutants in the ICL2. (A) B_{max} of mutant receptors in membrane of QBI-HEK293 cells determined by [^{3}H]5-CT binding. (B) B_{max} of mutant receptors in membrane of QBI-HEK293 cells determined by [^{3}H]SB269970 binding. Data are presented as receptor densities as percent of their respective controls (sister plates transfected with the wild-type 5-HT$_{7(a)}$ receptor)

3.5 Adenylyl cyclase assay

The adenylyl cyclase activity is measured by determining conversion of $[\alpha\text{-}^{32}P]$ATP to $[^{32}P]$cAMP in membrane preparations. G_s-coupled receptors and the 5-HT$_{7(a)}$ receptor regulate adenylyl cyclase activity, stimulating this enzyme.

The ability of the mutants in the TMH7 and in the ICL2 to activate adenylyl cyclase is also assayed, using the same ligands screened in the binding. The results obtained from the adenylyl cyclase assays are used to confirm the receptor's functionality measured as cAMP formed during the process.

In the TMH7 the mutant E366T and its derivates (E366R, E366A), R389D, Y374A and Y374T are very important for the receptor's activation. As shown in the binding results the receptors E366T and E366R have also totally lost the ability to activate the adenylyl cyclase. Similar results are showed with the mutant R389D where the receptor wasn't able to activate the adenylyl cyclase. While the mutants Y374A and Y374T showed after the mutations a differential change in affinity between agonist and antagonist ligands.

MUTANT	pEC50		pIC50
	5-CT	5-HT	SB269970
5-HT$_{7(a)}$	7,82 ± 0,07	7,06 ± 0,03	6,84 ± 0,09
W364V	7,99 ± 0,16	7,27 ± 0,12	6,49 ± 0,19
Y374A	7,62 ± 0,28	6,76 ± 0,04	6,36 ± 0,07
E366T	N.D.	N.D.	N.D.
E366R	N.D.	N.D.	N.D.
E366D	7,67	6,85	7,67
E366A	7,39	6,48	7,37
R367V	7,89	6,69	7,89
R389D	N.D.	N.D.	N.D.
D390K	7,69 ± 0,06	6,81 ± 0,10	6,78 ± 0,03

Table 6: Efficacy (EC$_{50}$) of 5-HT and 5-CT (agonists) and inhibiting efficacy (IC$_{50}$) of SB269970 to activate or inhibit adenylyl cyclase of membranes from QBI-HEK293 cells expressing 5-HT$_{7(a)}$ and the mutants in TMH7. Data are means ± S.E.M. from 2-3 experiments.
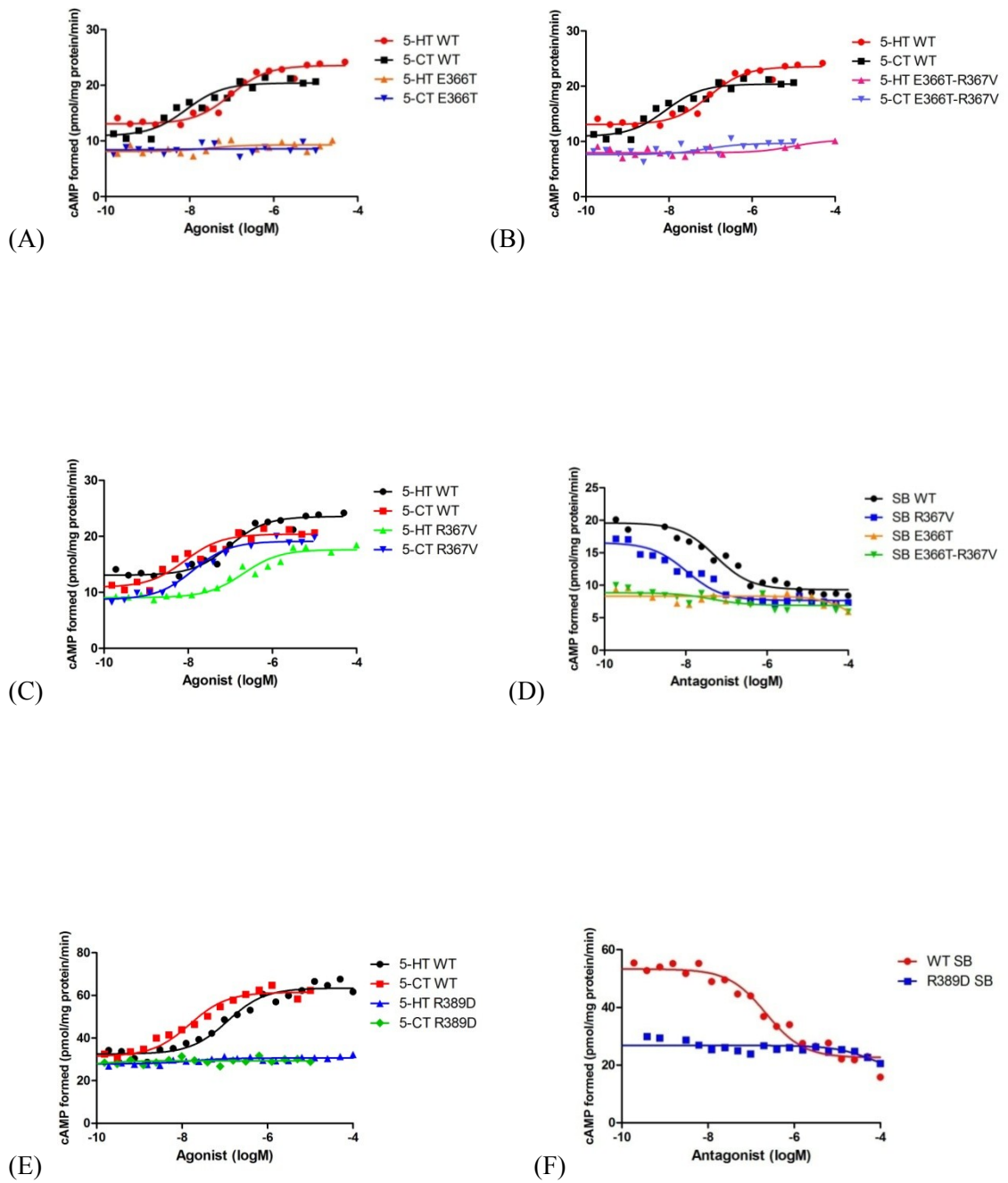
Fig.12: Adenylyl cyclase assay results from a single experiment: (A) on the mutant E366T, (B) the double mutant E366T-R367Vand (C) the R367V and with the agonists and (D) antagonist ligands; (E) the mutant R389D with the agonist ligands and (F) with the antagonist.
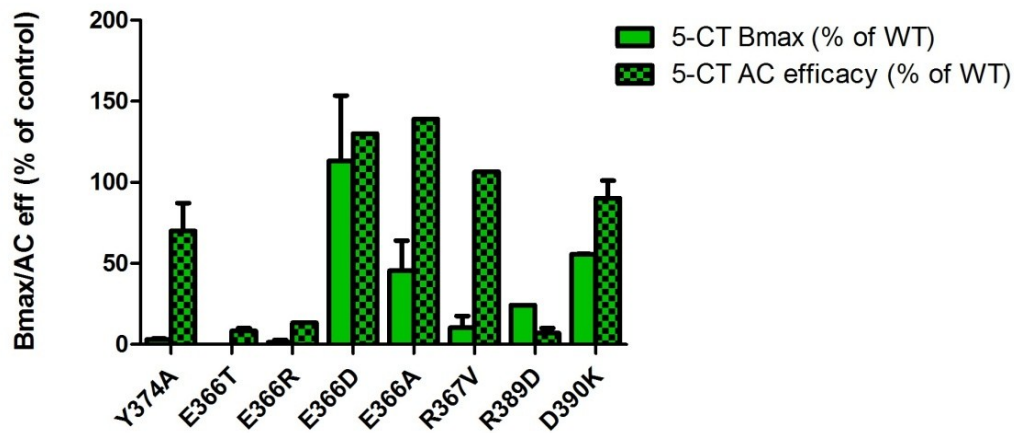
Fig.13: Comparison with the same ligand 5-CT between receptor densities (B_{max}) from binding assay and efficacy measured as adenylyl cyclase activity. Data are means ± S.E.M of 2-3 experiments.
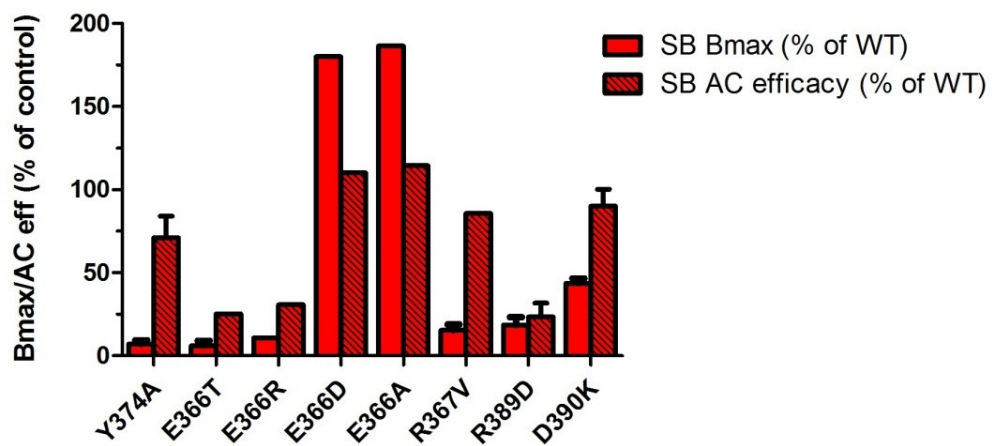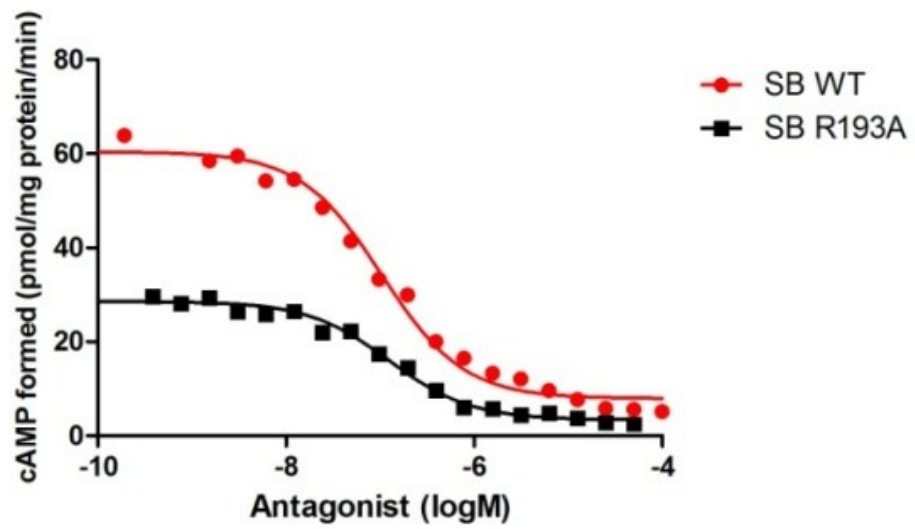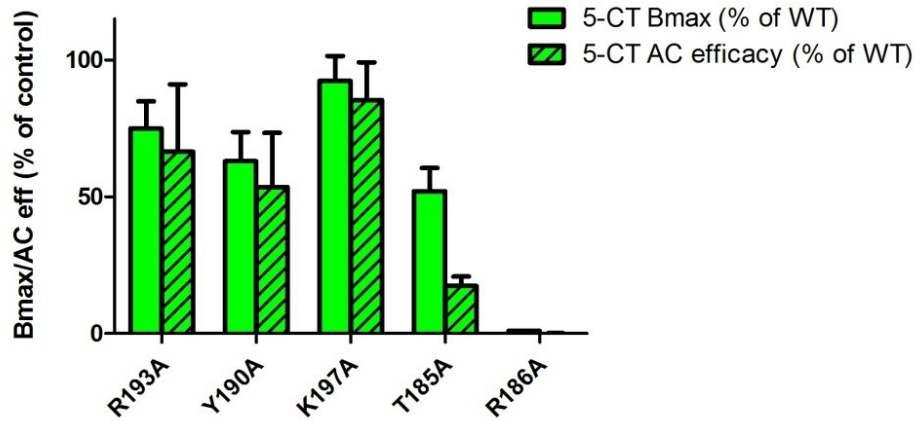

Fig.14: Comparison with the same ligand SB269970 between receptor densities (B_{max}) from binding assay and efficacy measured as adenylyl cyclase activity. Data are means ± S.E.M of 2-3 experiments.

The adenylyl cyclase assays performed on the mutants identified in the second intracellular loop showed interesting results. In particular two residues, Thr185 and Arg186, after the respectively mutation in Ala underlined an important reduction of the ability to activate the adenylyl cyclase in the first case and a totally loss of activation of the adenylyl cyclase with both ligands agonist and antagonist. Another mutant R193A showed only a partially reduction in the ability to activate the enzyme. The mutants Y190A and K197A didn't change the receptor's activity.

MUTANT	pEC50		pIC50
	5-CT	5-HT	SB269970
5-HT$_{7(a)}$	7,96 ± 0,06	7,30 ± 0,06	6,78 ± 0,08
Y190A	7,76 ± 0,11	7,10 ± 0,25	7,35 ± 0,20
R193A	8,24 ± 0,04	7,36 ± 0,15	6,63 ± 0,02
K197A	7,84 ± 0,27	7,09 ± 0,08	6,81 ± 0,15
R186A	N.D.	N.D.	N.D.
T185A	7,73 ± 0,30	6,82 ± 0,19	6,90 ± 0,16

Table 7: Efficacy (EC$_{50}$) of 5-HT and 5-CT (agonists) and inhibiting efficacy (IC$_{50}$) of SB269970 to activate or inhibit adenylyl cyclase of membranes from QBI-HEK293 cells expressing 5-HT$_{7(a)}$ and the mutants in second intracellular loop. Data are means ± S.E.M. from 2-3 experiments.
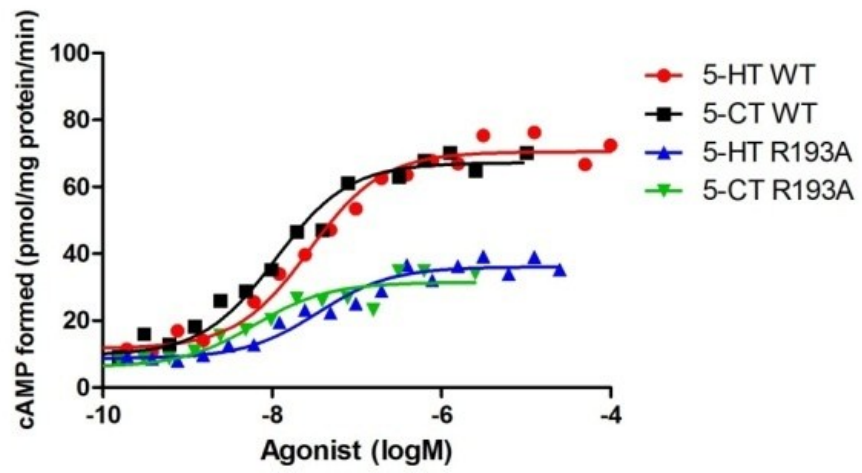
(A)

(B)

Fig.15: Adenylyl cyclase assay result on the mutant R193A with the agonists (A) and with the antagonist (B). Data are from one single experiment.
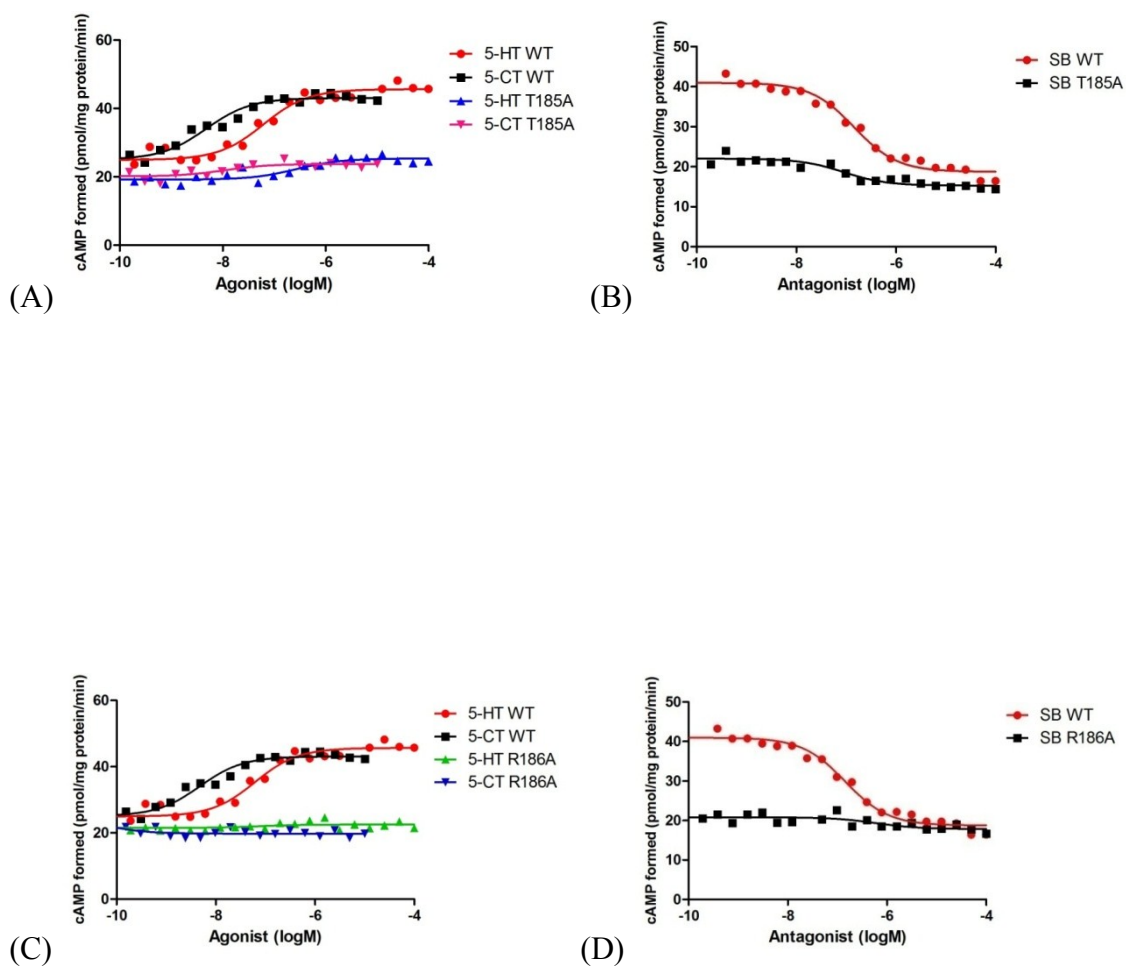
Fig.16: Adenylyl cyclase assay result on the mutant T185A with the agonist (A) and with the antagonist (B) and with the mutant R186A with the agonists (C) and (D) with the antagonist. Data are from one single experiment.

Fig.17: Comparison with the same ligand 5-CT between receptor densities (B_{max}) from binding assay and efficacy measured as adenylyl cyclase activity. Data are means ± S.E.M of 2-3 experiments
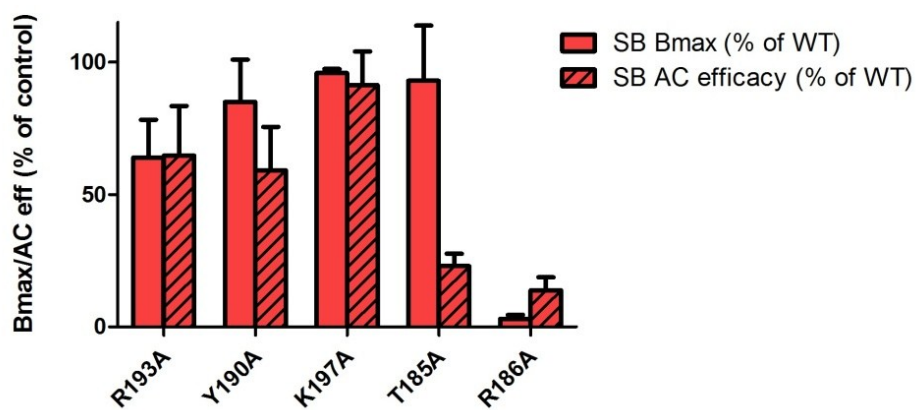
Fig.18: Comparison with the same ligand SB269970 between receptor densities (B_{max}) from binding assay and efficacy measured as adenylyl cyclase activity. Data are means ± S.E.M of 2-3 experiments

3.6 Western blotting analysis

The membrane preparations of each mutant created on the TMH7 and on the second intracellular loop are used to check the expression level of them and to confirm the functional results obtained in the previous assays, especially for those mutants that have changed, after the mutation, the receptor binding activity or the functional activity.

All membrane preparations are properly thawed and the samples are diluted to desired concentration using TE buffer. The Mini-PROTEAN Tetra Electrophoresis System (Bio-Rad) is prepared as described above to run the SDS-PAGE. When the run is finished the assembled sandwich is put in the transferring tank, containing the specific buffer, afterwards the membrane is incubated for the non-specific block in 10 ml of 5% non-fat dry milk in phosphate buffered saline (PBS)/Tween 20 (0.05 %) at room temperature for 1 hour. After which the membrane are incubated overnight at 4° C with 1/200 rabbit anti-5-HT$_7$R (Oncogene Research Products, Boston) in 5% milk-PBS/Tween 20.Thereafter, the blots were incubated with 1/5000 anti-rabbit, HRP-linked (Amersham ECL™-HRP Linked Secondary Antibodies, GE Healthcare) for 1 hour at room temperature in 5% milk-PBS/Tween 20. The membrane are developed using theLumiGLOChemiluminescent Substrate kit.
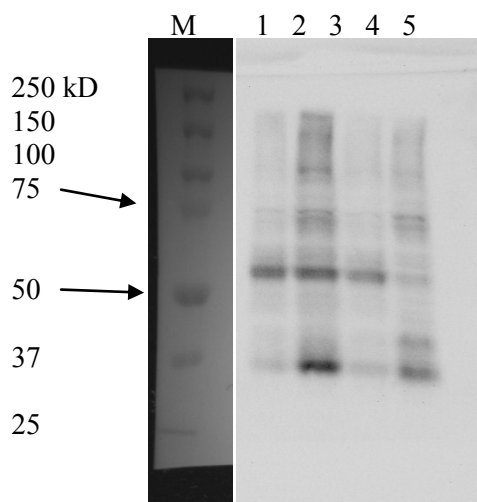
Fig.19: Relative molecular mass of the 5-HT$_{7(a)}$ receptor and mutants created. The 5HT$_7$ receptor also has putative sites for N-linked glycosylation and phosphorylation which may lead to variations in observed molecular weights. The 5HT$_7$ antibody recognizes all described 5HT$_7$ receptor splice variants. M: precision plus protein dual color standards; well 1: 5-HT$_{7(a)}$ wild-type; 2: mutant E366T; 3: mutant R389D; 4: mutant Y374A and in the well 5: negative control constituted by the empty plasmid used in the cloning procedure

3.7 Molecular Dynamics

35 ns and 31 ns molecular dynamics simulations of the 5-HT$_7$ and 5-HT$_{1a}$ serotonergic receptors embedded in a POPC bilayer were carried out at 35 ns and 31 ns respectively. Systems were hydrated with explicit water molecules.Na$^+$ and Cl$^-$ ions were added to reach the physiologic ionic concentration of 150 mM. No differences were in adding NaCl or KCl because the "only charge based parameterization" of CHARMM is the same for both the cations Na$^+$ and K$^+$.

The simulation was stopped when the proteins reached the conformational equilibrium. Because the G-protein binding domains of both GPCRs have a great flexibility during simulations the RMSD (Root Mean Square Deviation) of the corresponding transmembrane domain was calculated.
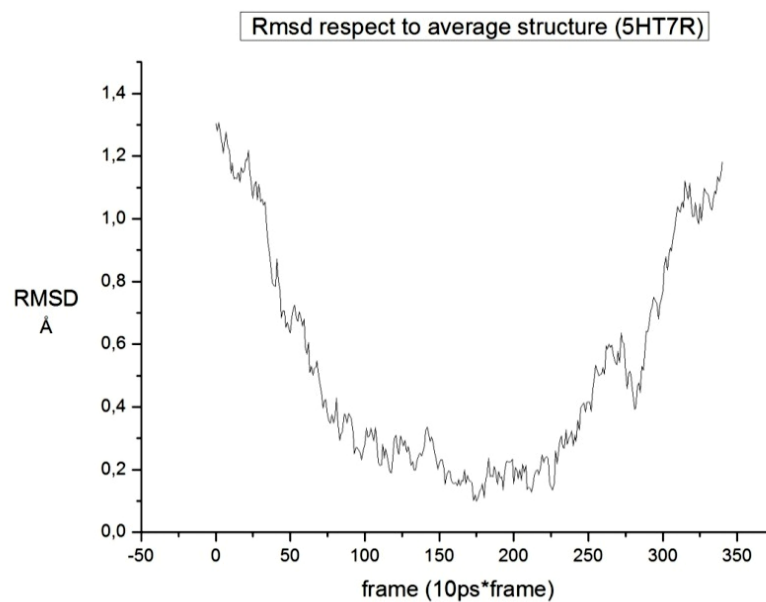
Fig.20: RMSD of the 5-HT$_7$ receptor compared to the average structure during 35 ns of simulation.

The 5-HT$_7$ receptor reached a stable conformational equilibrium between 7.5 ns and 25 ns.The RMSD (fig. 20) of the 5-HT7Rshows a conformationalinstabilitywhich mayreflect the highconstitutive activity.
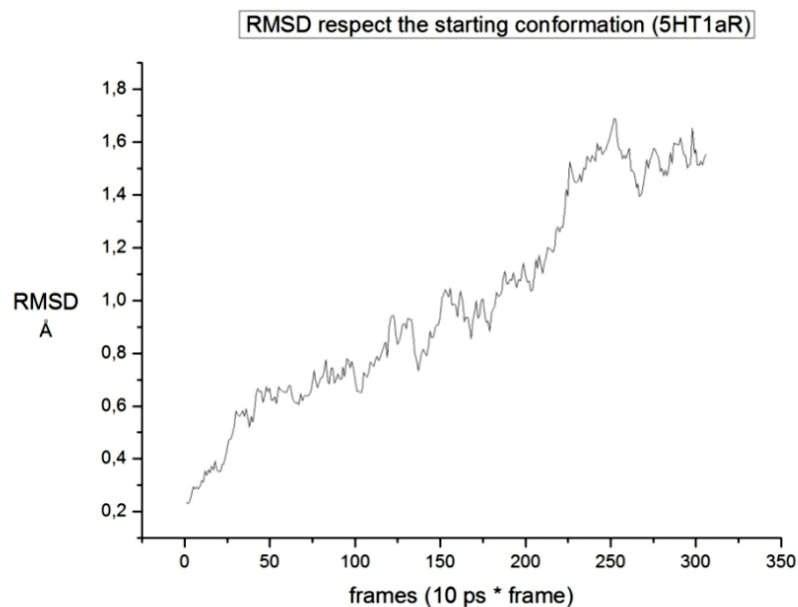
Fig.21: RMSD profile of the 5-HT1A receptor compared to the starting structure during 31 ns of simulation.

The structural deviation (fig. 21) when compared to the starting structure reaches a plateau at 225 ps approaching the end of the simulation. RMSD profiles of the two receptors are in agreement with a different dynamic behavior, suggesting that they map a different conformational space.

Moreover the two receptors show structural differences after the simulations in membrane environment.

The RMSD was assessed by superimposition of the two receptors before and after the simulations. It increases from 1.96 to 2.53 Å. This means that the two receptor

differentiate in structure due to the simulation in membrane. Moreover the binding sites of the two receptors are different in shape and dimensions (fig. 22).
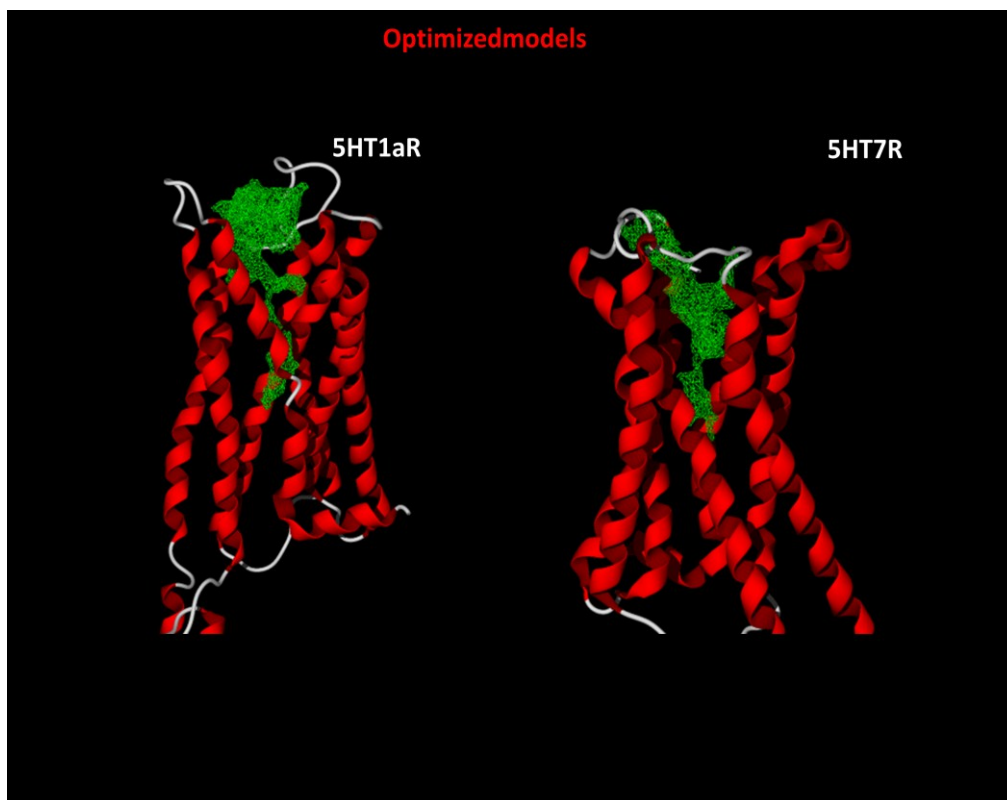
Fig. 22: Binding sites of 5-HT$_{1a}$ and 5-HT$_7$ after respectively 31 and 35 ns of simulation in membrane environment.

After these preliminary simulations on the 5-HT$_7$ receptor some important mutants are analyzed with the same procedure.

The results of directed mutagenesis on Glu366 (helix VII) residue have showed a loss of receptor's activity after the mutation in Thr and Arg.Glu366 forms an high stable salt bridge with Arg350 (helix VI) as shown in the figure 23.
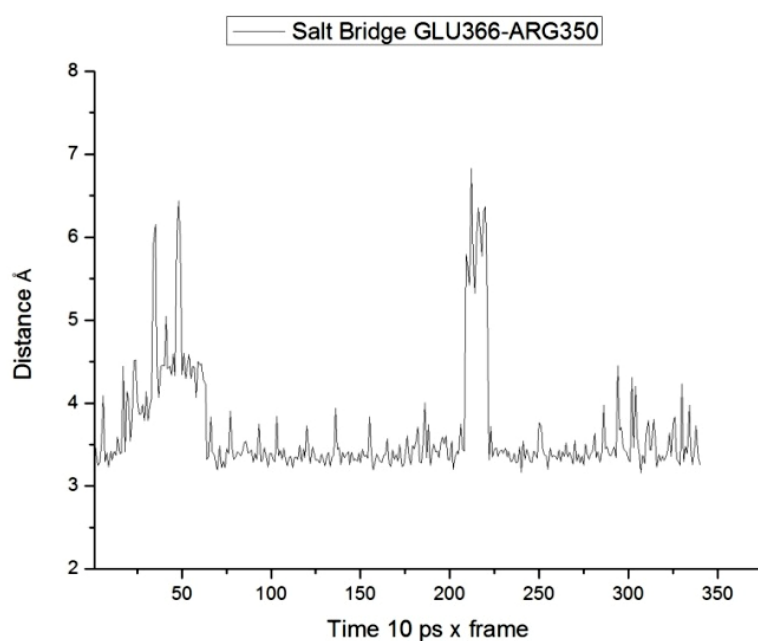
Fig. 23. Salt bridge formation between Glu366 and Arg350.

The residue Arg367 interacts with Asp142 (belonging to 2th helix of 5-HT7) by a high stable salt bridge (fig.24). This residue mutated in Val showed a partial reduction in the binding fuction.
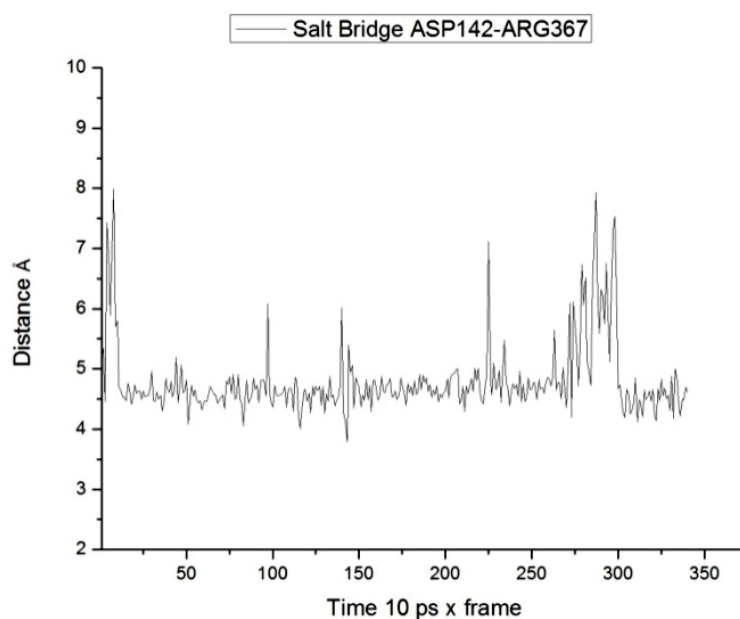
Fig.24: Salt bridge formation between Asp 142 and Arg 367

The salt bridge Arg367-Asp142 is partially instable (0.8 % of whole simulation), due to the formation of a three members salt bridge Arg367-Glu366-Arg350 which is stable till 30 ps.Helix VII at the extracellular site interact by two salt bridges with helix II and helix VI as showed in figure 25.
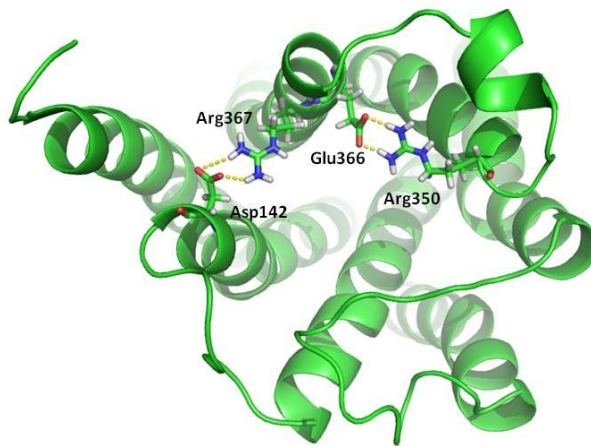
Fig. 25: Salt bridge network between Helix II-Helix VII-Helix VI of 5-HT7 receptor.

The residue Tyr374 mutated in Ala showed a differential change in affinity between agonist and antagonist ligands, this could be due to the electrostatic interaction with Asp162 (fig. 26).
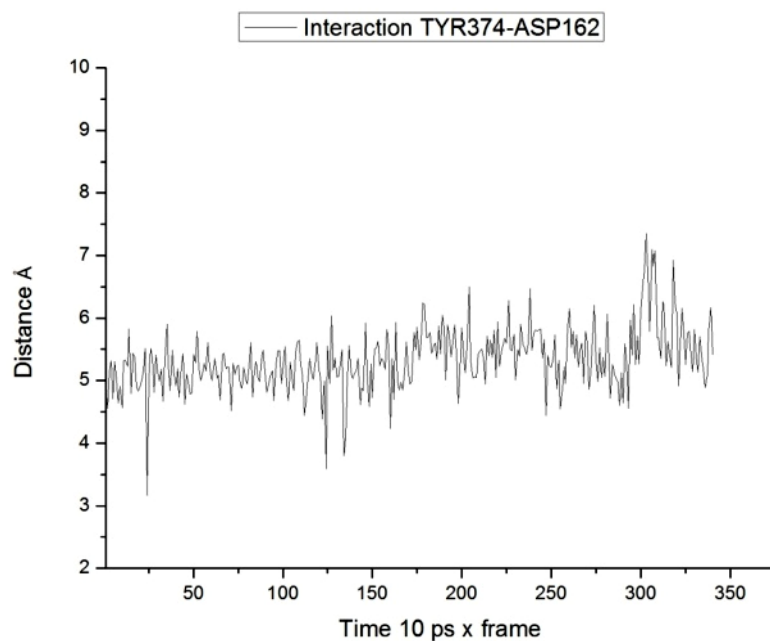
Fig. 26. Electrostatic interaction between Tyr 374 and Asp 162.

The residue Arg389 in helix VII after the mutation in Asp pointed out an important result for the localization of the activation site of the receptor. The new receptor reduced partially the binding with the agonist and antagonist ligands, but wasn't able to bind the G-protein to activate the adenylyl cyclase.

This residue points toward the water during simulation; its position is at the base of helix VII and near the G protein binding domain. Thus the mutagenesis data on this residue might be explained with a lack of important interaction pattern with the G protein and we can assume that the charge is important.
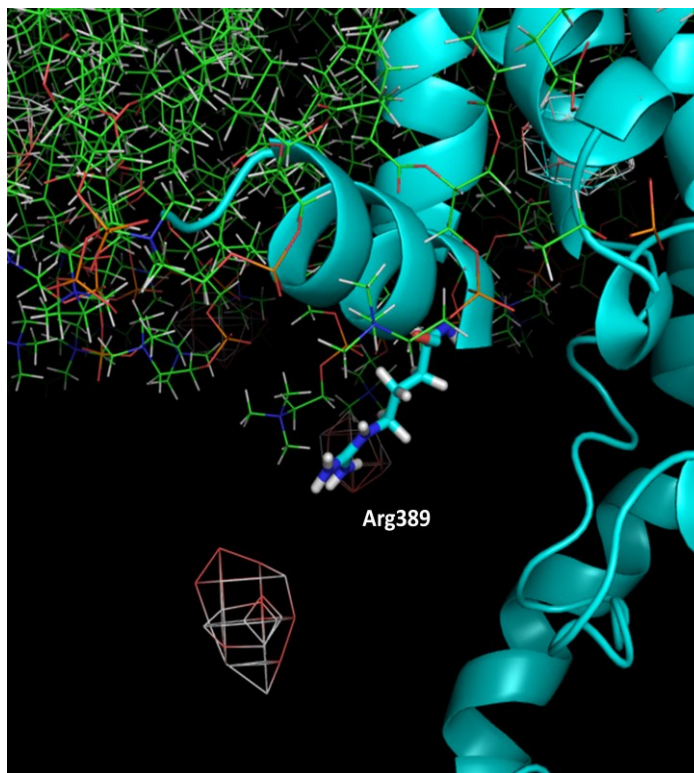
Fig. 27: Arg389 at membrane-water interface. The interaction with a G-protein is showed.

3.8 Molecular Docking

The most important residue in the TMH7 analyzed with some molecular docking procedure is the Tyr374. This residue was mutated at the beginning in Ala and then in Thr, the result from the functional assays showed in both cases a differential change in affinity between the different classes of ligands. Using the molecular docking software MoleGro, the 5-HT$_{7(a)}$ receptor (wild-type) and the two mutants (Y374A and Y374T) are analyzed to explain these results.

The ligands used in the docking procedure are: 5-CT, 5-HT and SB269970 (antagonist of the serotonin).

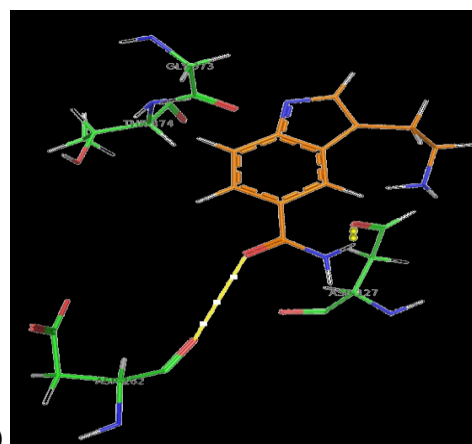With the ligand 5-CT the docking result (fig.28) showed that:

- The 5-HT$_{7(a)}$ (wild-type) receptor binds the ligand with the Asp127, Cys165, Cys166, Gly373, Ser169

- In the mutant Y374A the ligand performed some electrostatic interaction with Asp162, Asp127

- In the mutant Y374T the ligand bind the receptor by means of Asp127, Asp162
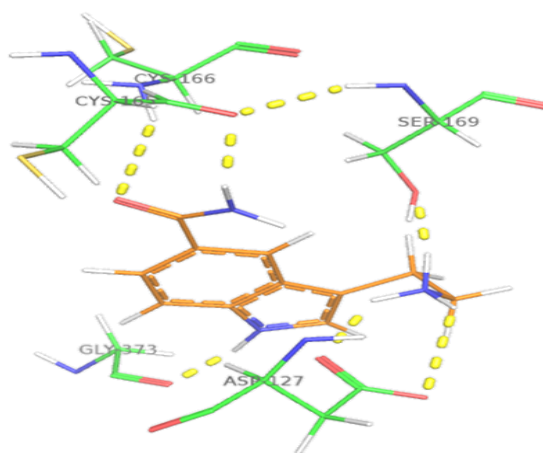
(A)
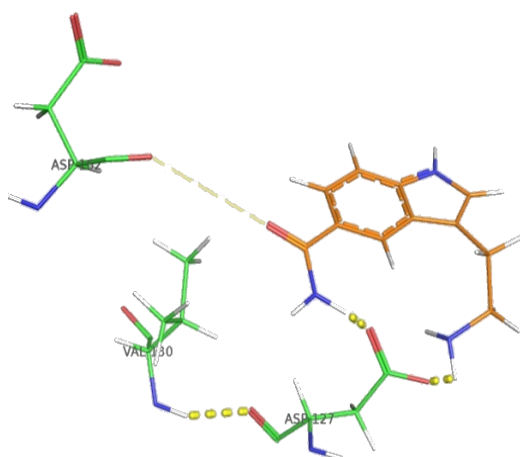
(B)

(C)

Fig.28: Molecular docking results with the ligand 5-CT on the wild-type (A), Y374A (B) and Y374T (C)

The ligand 5-HT binds with (fig.29):

- The wild-type binds through the residues Asp127, Asp162, Ala126Tyr374 and Ser377
- The mutant Y374A binds through the Asp127, Asp162 and Ser377
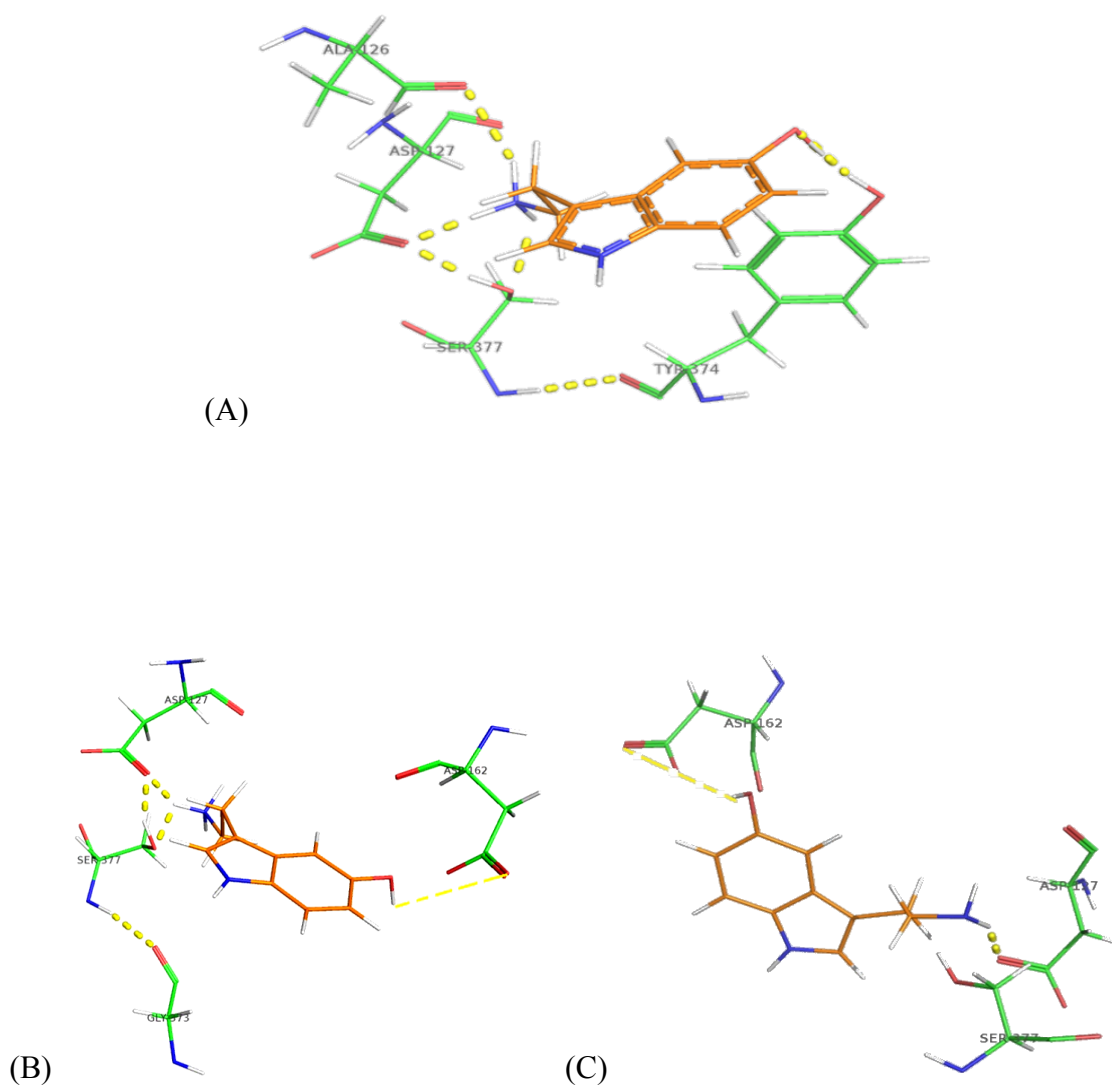- The mutant Y374T binds the residues Asp162, Asp 127 and Ser 377

(A)

(B)

(C)

Fig.29: Molecular docking results with the ligand 5-HT on the wild-type (A), Y374A (B) and Y374T (C)

The antagonist SB269970 binds (fig.30):

- The wild-type through the Asp162 and Tyr374 with the OH-group and Ser377
- The Y374A with Asp162 ser347
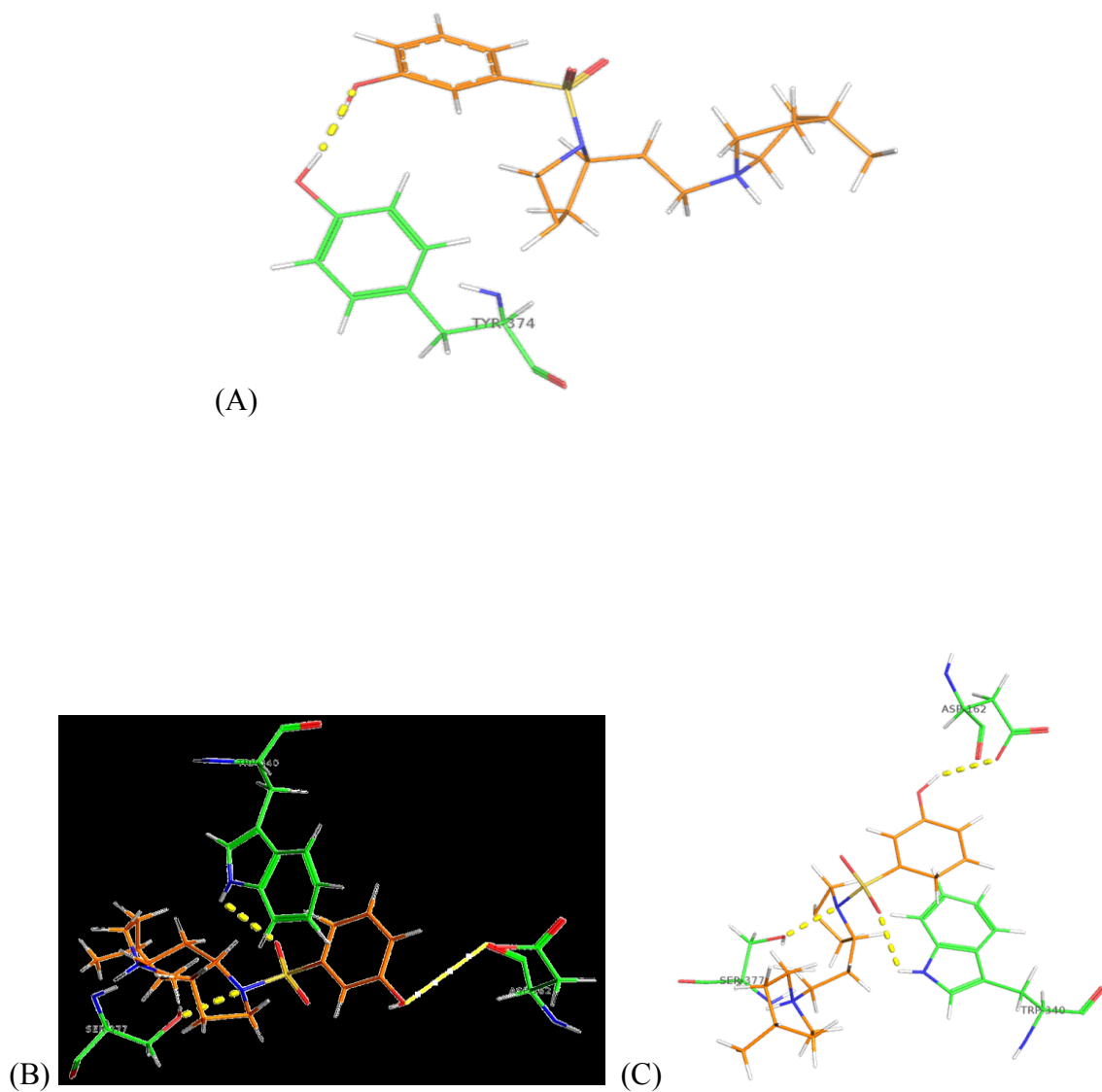- The mutant Y374T interacts with Asp162, Ser347, Gln235 and Thr167

(A)

(B)

(C)

Fig.30: Molecular docking results with the ligand SB269970 on the wild-type (A), Y374A (B) and Y374T (C)

These results shows that the wild-type receptor with both agonist and antagonist ligands interacts with residues located in the 7th helix of the receptor. The mutants bind the agonist ligands in a binding cavity located towards the 7th helix, while the antagonist SB269970 interacts with the receptor in a binding cavity towards the helices II-III-IV-V.

4 DISCUSSION AND CONCLUSION

The present project shows the importance of some amino acid residues located in the 7th transmembrane helix (hypothetical binding site with the ligands) and in the second intracellular loop (hypothetical activation site with the G-protein) of the 5-HT$_{7(a)}$ receptor.

The mutagenesis studies on these two different parts of the 5-HT$_{7(a)}$ receptor underline the importance of specific residues in the TMH7 as the Glu366, Arg367 (7.36), Tyr374 (7.43) and Arg389, and in the second intracellular loop as Thr185 and Arg186.

The functional results obtained on the Glu366 and Arg367 after the respectively mutations show that the creation of a specific salt bridge network between Helix II-Helix VII-Helix VI of the 5-HT$_{7(a)}$ receptor is very important to establish the receptor's activity, and the presence of the specific charges on the amino acid mentioned above are necessary to bind the different classes of ligands.

The work by Kolaczkowski M. et al. (2006) are very interesting to explain our results on the mutants of the TMH7. They underlined that each docked ligand not only "found" its own best position and geometry in the receptor, but also "chose" the most convenient conformation of the binding site. The positioning of most of the ligands within a receptor binding site was analogous to the binding mode predicted in their earlier study for arylpiperazine derivatives and their structural analogues (ergolines and aporphines) in 5-HT1AR. The dockings superimposed an arylpiperidine/arylpiperazine or β-carboline moiety on an ergoline, aporphine, or tricyclic fragment and placed all of them in the pocket between TMHs 4-6, while amide/imide or sulfonamide moieties were located in the region occupied by an amide fragment of ergoline derivatives (a pocket between TMHs 7-3). In the other studies, an opposite placement was presented: the amide moieties of arylpiperazines or arylsulfonamide fragments were superimposed (without receptor structure) on an ergoline, aporphine, or tricyclic moiety and were then manually positioned in the cavity between TMHs 4-6. The aboveambiguity may be due to the fact that ligand-ligand superimposition assumes one common binding pocket for all compounds and that there is a fair symmetry of the 5-HT7R binding site. The

concept of different binding modes and binding sites resulted from the applied receptor based approach and substantially influenced the pharmacophore model for 5-HT7R antagonism, especially the "selectivity" hypothesis.

The "affinity" pharmacophore presented is fairly general and has a lot in common with other pharmacophores for monoamine receptors, as it was also generated using nonselective ligands showing a multireceptor profile. It defines features (and their combinations) that may afford 5-HT7R antagonism, irrespective of the selectivity over other targets. On the other hand, the "selectivity" pharmacophore was basedon selective antagonists only and is an attempt to describe the features providing exclusive affinity for 5-HT7R. A key to selectivity lies in the differences between biological targets that are "recognized" by ligands upon binding. As mentioned in the introduction, the 5-HT7R model was built using the methodology developed for 5-HT1AR as a result of the high structural similarity and common ligands. The superimposition of both binding sites reveals that among the amino acids having van der Waals contacts with ligands, only three residues are different: Glu7.35(5-HT7R)-Gly (5-HT1AR), Arg7.36-Ala, and Leu7.39-Asn. Sequence analysis of the putative binding sites of some other monoamine receptors, for which nonselective 5-HT7R antagonists display affinity (5-HT2A, D2, R1), also indicates a certain similarity, especially in the binding cavity between TMHs 4-6. Like in the case of 5-HT1AR, differences occur mainly in the pocket formed by TMHs 7-3 (residues 7.35, 7.36, 7.39 and 2.60, 2.61, 2.64, 2.65). This is in line with the observation that 5-HT7R antagonists that enter into important, specific interactions with the residues from the TMHs 7-3 pocket (especially non conserved Arg7.36) are predominantly more selective than those anchoring mainly between TMHs 4-6.The presence and the quality of AR1 feature is of great importance here, because it assures specific interactions with Phe3.28 and Arg7.36. The geometry of the terminal amide/imide/sulfonamide fragment (a mutual arrangement of the aryl ring, AR1, and the carbonyl oxygen, HBA1) substantially influences 5-HT7R affinity and/or selectivity by appropriately fitting the above-mentioned residues and Tyr7.43. Arylsulfonamidoalkylamines possess optimal geometry, which allows their simultaneous π-π stacking with Phe3.28, ion-π interaction with Arg7.36, and H-bonding with Tyr7.43. These interactions (together with a salt bridge to Asp3.32) make them independent of specific interactions with the aromatic residues from TMHs 4-6.Substitution of the aromatic moiety (AR2) in the 4-position of the piperidine ring

allowing specific interactions with the pocket between TMHs 4-6, does not influence 5-HT7R affinity, but increases (by 1-2 orders of magnitude) the affinity for some other monoamine receptors.

The ability of a ligand to enter into dominating interactions within the TMHs 7-3 pocket is not the only way to selective antagonism, because some selective compounds were accommodated by the cavity between TMHs 4-6. The selectivity, in this case, is possible probably due to spatial differences between the receptors. And in particular the "selectivity" hypothesis emphasized the role of the presence and geometry of aromatic (AR1) and H-bond accepting (HBA1) moieties interacting with a less conserved part of the binding site localized between TMHs 7and 3 in providing selectivity over other monoamine GPCRs.

Receptor is kept in an inactive state until the binding of a ligand "agonist" switches them into an active state within milliseconds. The transition between the inactive and active states involves the release of at least two important molecular constraints, known as the "ionic lock" between charged residues at the cytosolic sides of the receptor and the "rotamer toggle switch" in helix 6. Yao et al. 2006 report a fluorescence method for following the breaking of the ionic lock in the β_2-adrenergic receptor (β_2AR), and identify agonists that differentially affect the two molecular switches. The β_2-adrenergic receptor is a well-characterized receptor that serves as a model for dissecting mechanism of activation of rhodopsine-like class A GPCRs. The keystone in the overall process of activating these receptors is a structural rearrangement of several transmembrane helices, in particular helices 3 and 6, triggered by presumably conserved switches that involve the disruption of an ionic interaction between the cytoplasmic face of helix 3 and helix 6 (ionic lock) and a rotamer toggle switch (modulation of the helix conformation around a conserved proline-kink) in helix 6. These transmembrane movements expose receptor epitopes at the cytosolic side that should drive heterotrimeric G protein signaling. Ligands that bind to GPCRs may show different efficacies in activating a specific receptor, thereby eliciting full or partial receptor responses.

Ballesteros et al. 2001established that the TM3 and TM6 play a role in GPCR activation. The DRY motif at the cytoplasmic side of TM3 is highly conserved throughout the subfamily of rhodopsin-like GPCRs. Glu-268 (6.30) at the cytoplasmic side of TM6 is also highly conserved among multiple rhodopsin-like GPCRs including

most neurotransmitter receptors, the glycoprotein hormone receptors, the opsins, and rhodopsin. Mutation of the arginine (Arg3.50) has established an important role of this residue in G-protein activation. Previous studies have also indicated a critical function of the adjacent aspartic acid (Asp3.49) for receptor activation. A network of interactions among Asp/Glu3.49, Arg3.50, and Glu6.30 maintains the cytoplasmic ends of these two helices immobilized in the inactive state of the receptor and, thus, may constitute a switch mechanism that is important for the activation of many rhodopsin-like GPCRs. Ballesteros et al. 1998proposed that the ionic counterpart of Arg3.50 in the inactive state could be the adjacent Asp3.49, and that in the active state Asp3.49 is protonated, and Arg3.50 interacts instead with Asp2.50. They have hypothesized that in the inactive state, Arg3.50 not only interacts with Asp3.49 but also with Glu6.30, and that this ionic interaction between the cytoplasmic ends of TM6 and TM3 is an ionic lock maintaining the receptor in the inactive state.

These studies found in literature can explain the results obtained with the mutations performed on the Thr185 and Arg186 in the second intracellular loop. These residues are very close to the conserved DRY motif, and probably are involved in the activation mechanism. The partial or complete loss of receptor's activation after the mutations can be explained as a loss of amino acids with specific chemical features (positively charged and polarity) both necessary to switch the receptor in the active state. The next studies of molecular dynamics and molecular docking on these residues can help us to understand how the ligands regulate the receptor's activation and what is the specific structural conformation that the receptor uses to bind the G- protein and to activate the adenylyl cyclase that will produce the specific intracellular signal.

If the next studies will give interesting results we can define the specific binding pocket and the specific activation site of the 5-HT$_{7(a)}$ receptor and we can use this information to find new drug able to react with the receptor and available for new pharmacological treatment.

5 REFERENCE LIST

Andressen KW, Norum JH, Levy FO, Krobert KA. "Activation of adenylyl cyclase by endogenous G(s)-coupled receptors in human embryonic kidney 293 cells is attenuated by 5-HT(7) receptor expression." *Mol. Pharmacol*, 2006: 69: 207-215.

Baker LP, Nielsen MD, Impey S, Metcalf MA, Poser SW, Chan G, Obrietan K, Hamblin MW, Storm DR. "Stimulation of type 1 and type 8 Ca2+/calmodulin-sensitive adenylyl cyclase by the Gs-coupled 5-hydroxytryptamine subtype 5-HT7A receptor." *J.Biol. Chem*, 1998: 273: 17469-17476.

Ballesteros J, Kitanovic S, Guarnieri F, Davies P, Bernard JF, Konvicka K, Chi L, Millar RP, Davidson JS, Weinstein H, Sealfon SC. "Funtional microdomains in G-protein-coupled receptors. The conserved arginine-cage motif in the gonadotropin-releasing hormone receptor." *The Journal of Biological Chemistry*, 1998: 273, 10445-10453.

Ballesteros JA, Jensen AD, Liapakis G, Rasmussen SGF, Shi L, Gether U, Javitch JA. "Activation of the beta-Adrenergic Receptor Involves Disruption of an Ionic Lock between the Cytoplasmic Ends of Transmembrane Segments 3 and 6." *The Journal of Biological Chemistry*, 2001: Vol 276,No.31- 29171-29177.

Bockaert J, Pin JP. «Molecular tinkering of G protein-coupled receptors: an evolutionary success.» *EMBO J.*, 1999: 18: 1723-1729.

Cabrera-Vera TM, Vanhauwe J, Thomas TO, Medkova M, Preininger A, Mazzoni MR, Hamm HE. «Insights into G protein structure, fuction and regulation.» *Endocr. Rev.*, 2003: 24: 765-781.

Cooper, DM. «Regulation and organization of adenylyl cyclase and cAMP.» *Biochem. J.*, 2003: 375: 517-529.

Costa T, Herz A. «Antagonists with negative activity at delta opioid receptors coupled to GTP-binding proteins.» *Proc. Natl.Acad.Sci. U.S.A.*, 1989: 86: 7321-7325.

De Lean A, Stadel J, Lefkowitz R. "A ternary complex model explain the agonist-specific binding properties of the adenylate cyclase-coupled beta-adrenergic receptor." *J. Biol. Chem.*, 1980: 255, 7108-7117.

de Ligt RA, Kourounakis AP, IJzerman AP. «Inverse agonism at G protein-coupled receptors: (patho)physiological relevance and implications for drug discovery.» *Br. J. Pharmacol*, 2000: 130: 1-12.

De Martelaere K, Lintermans B, Haegeman G, Vanhoenacker P. «Novel interaction between the human 5-HT7 receptor isoforms and PLAC-24/eIF3k.» *Cell. Signal.*, 2007a: 19: 278-288.

Frishman W, Grewall P. "Serotonin and the heart." *Ann. Med.*, 2000: 32, 195-209.

Galadrin S, Oligny-Longpre G, Bouvier M. «The evasive nature of drug efficacy: implications for drug discovery.» *Treds Pharmacol. Sci*, 2007: 28: 423-430.

Gellynck E, Laenen K, Andressen KW, Lintermans B, De MK, Matthys A, Levy FO, Hegeman G, Vanhoenacker P, Van CK. «Cloning, genomic organitazion and functionality of 5-HT(7) receptor splice variants from mouse brain.» *Gene*, 2008: 426: 23-31.

Gether U, Kobilka BK. «G protein-coupled receptors. II. Mechanism of agonist activation.» *J.Biol.Chem*, 1998: 273: 17979-17982.

Gloerich M, Bos JL. «Epac: defining a new mechanism for cAMP action.» *Annu.Rev.Pharmacol.Toxicol.*, 2010: 50: 355-375.

Guthrie CR, Murray AT, Franklin AA, Hamblin MW. «Differential agonist-mediated internalization of the human 5-hydroxytryptamine 7 receptor isoforms.» *J.Pharmacol.Exp.Ther*, 2005: 313: 1003-1010.

Hedlund PB, Sutcliffe JG. «Functional, molecular and pharmacological advances in 5-HT7 receptor research.» *Trends Pharmacol.Sci*, 2004: 25: 481-486.

Heidmann DE, Metcalf MA, Kohen R, Hamblin MW. «Four 5-hydroxytryptamine7 (5-HT7) receptor isoforms in human and rat produced by alternative splicing: species differences due to altered intron-exon organization.» *J.Neurochem.*, 1997: 68: 1372-1381.

Hoyer D, Clarke DE, Fozard JR, Hartig PR, Martin GR, Mylecharane EJ, Saxena PR, Humphrey PP. «International Union of Pharmacology classification of receptor for 5-hydroxytryptamine (Serotonin).» *Pharmacol.Rev.*, 1994: 46: 157-203.

Hoyer D, Hannon JP, Martin GR. «Molecular, pharmacological and functional diversity of 5-HT receptors.» *Pharmacol.Biochem.Behav*, 2002: 71: 533-554.

Hurley, JH. «Structure, mechanism, and regulation of mammalian adenylyl cyclase.» *J.Biol.Chem*, 1999: 274: 7599-7602.

Ji TH, GrossmannM, Ji I. «G protein-cupled receptors. I. Diversity of receptor-ligand interactions.» *J.Biol.Chem*, 1998: 273: 17299-17302.

Kaumann AJ, Levy FO. "5-hydroxytryptamine receptors in the human cardiovascular system." *Pharmacol. Ther.*, 2006: 111, 674-706.

Kenakin, T. «Efficacy at G-protein-coupled receptors.» *Nat.Rev.Drug Discov.*, 2002: 1: 103-110.

Kolaczkowski M, Nowak M, Pawlowski M, Bojarski AJ. "Receptor-Based Pharmacophores for Serotonin 5-HT7R Antagonists-Implications to Selectivity." *J. Med. Chem*, 2006: 49, 6732-6741.

Krobert KA, Andressen KW, Levy FO. «Heterologous desensitization is evoked by both agonist and antagonist stimulation of the human 5-HT(7) serotonin receptor.» *Eur.J.Pharmcol.*, 2006: 532: 1-10.

Krobert KA, Bach T, Syversveen T, Kvingedal AM, Levy FO. «The cloned human 5-HT7 receptor splice variants: a comparative characterization of their pharmacology, function and distribution.» *Naunyn Schmiedebergs Arch.Pharmacol*, 2001: 363: 620-632.

Krobert KA, Levy FO. «The human 5-HT7 serotonin receptor variants: costitutive activity and inverse agonist effects.» *Br.J.Pharmacol*, 2002: 135: 1563-1571.

Kvachnina E, Dumuis A, Wlodarczyk J, Renner U, Cochet M, Richter DW, Ponimaskin E. «Constitutive Gs-mediated, but not G12-mediated, activity of the 5-hydroxytryptamine 5-HT7(a) receptor is modulated by the palmitoylationof its C-terminal domain.» *Bioche.Biophys.Acta*, 2009: 1793: 1646-1655.

Kvachnina E, Liu G, Dityatev A, Renner U, Dumuis A, Richter DW, Dityateva G, Schachner M, Voyno-Yasenetskaya TA, Ponimaskin EG. «5-HT7 receptor is coupled to G alpha subunits of heterotrimeric G12-protein to regulate gene transcription and neuronal morphology.» *J. Neurosci.*, 2005: 25: 7821-7830.

Leff, P. "The two-state modelof receptor activation." *Trends Pharmacol. Sci.*, 1995: 16, 89-97.

Lohse MJ, Benovic JL, Caron MG, Lefkowitz RJ. «Multiple pathways of rapid beta 2-adrenergic receptor desensitization. Delineation with specific inhibitors.» *J.Biol.Chem*, 1990: 265: 3202-3211.

Milligan G, Kostenis E. «Heterotrimeric G-proteins: a short history.» *Br.J.Pharmacol.*, 2006: 147 Suppl1: S46-S55.

Moore CA, Milano SK, Benovic JL. «Regulation of receptor trafficking by GRKs and arrestins.» *Annu.Rev.Physiol.*, 2007: 69: 451-482.

Norum JH, Methi J, Mattingly RR, Levy FO. «Endogenous expression and protein kinase A-dependent phosphorylation of the guanine nucleotide exchange factor Ras-GRF1 in human embryonic kidney 293 cells.» *FEBS J.*, 2005: 272: 2304-2316.

Paing MM, Johnston CA, Siderovski DP, Trjo J. «Clathrin adaptor AP2 regulates thrombin receptor constitutive internalization and endothelial cell resensitization.» *Mol.Cell.Biol*, 2006: 26: 3231-3242.

Paing MM, Temple BR, Trejo J. «A tyrosine-based sorting signal regulates intracellular trafficking of protease-activated receptor-1: multiple regulatory mechanisms for agonist-induced G protein-coupled receptor internalization.» *J.Biol.Chem*, 2004: 279: 21938-21947.

Perez DM, Karnik SS. «Multiple signaling states G-protein-coupled receptors.» *Pharmacol.Rev.*, 2005: 57: 147-161.

Pierce KL, Premont RT, Lefkowitz RJ. «Seven-transmembrane receptors.» *Nat.Rev.Mol.Cell Biol*, 2002: 3: 639-650.

Roth BL, Craigo SC, Choudhary MS, Uluer A, Monsma FJ, Jr Shen Y, Meltzer HY, Sibley DR. «Binding of typical and atypical antipsychotic agents to 5-hydroxytryptamine-6 and 5-hydroxytryptamine-7 receptors.» *J.Pharmacol.Exp.Ther.*, 1994: 268: 1403-1410.

Ruat M, Traiffort E, Leurs R, Tardivel-Lacombe J, Diaz J, Arrang JM, Schwartz JC. «Molecular cloning, characterization, and localization of a high-affinity serotonin receptor (5-HT7) activating cAMP formation.» *Proc.Natl.Acad.Sci.U.S.A.*, 1993: 90: 8547-8551.

Samama P, Cotecchia S, Costa T, Lefkowitz R. "A mutation-induced activated state of the beta-adrenergic receptor. Extending the ternary complex model." *J. Biol. Chem.*, 1993: 268, 4625-4636.

Seifert R, Wenzel-Seifert K. «Constitutive activity of G-protein-coupled receptors: cause of disease and common property of wild-type receptors.» *Naunyn Schmiedebergs Arch.Pharmacol*, 2002: 366: 381-416.

Simonds, WF. «G protein regulation of adenylate cyclase.» *Trends Pharmacol.Sci.*, 1999: 20: 66-73.

Simonin F, Karcher P, Boeuf JJ, Matifas A, Kieffer BL. «Identification of a novel family of G protein-coupled receptor associated sorting proteins.» *J.Neurochem.*, 2004: 89: 766-775.

Smith C, Rahman T, Toohey N, Mazurkiewicz J, Herrick-Davis K, Teitler M. «Risperidone irreversibly binds to and inactivates the h5-HT7 serotonin receptor.» *Mol.Pharmacol.*, 2006: 70: 1264-1270.

Strange, PG. «Mechanisms of inverse agonism at G-protein-coupled receptors.» *Trends Pharmacol.Sci.*, 2002: 23: 89-95.

Tang WJ, Hurley JH. «Catalytic mechanism and regulation of mammalian adenylyl cyclases.» *Mol.Pharmacol.*, 1998: 54: 231-240.

Teitler M, Toohey N, Knight JA, Klein MT, Smith C. «Clozapine and other competitive antagonists reactivate risperidone-inactivated h5-HT(7) receptors: radioligand binding and functional evidence for GPCR homodimer protomer interactions.» *Psychopharmacology (Berl)*, 2010.

Urban JD, Clarke WP, von Zastrow M, Nichols DE, Kobilka B, Weinstein H, Javitch JA, Roth BL, Christopoulos A, Sexton PM, MIller KJ, Spedding M, Mailman RB. «Functional selectivity and classical concepts of quantitative pharmacology.» *J.Pharmacol.Exp.Ther.*, 2007: 320: 1-13.

Vaidehi N, Kenakin T. «The role of conformational ensembles of seven transmembrane receptors in functional selectivity.» *Curr.Opin.Pharmacol.*, 2010.

Vanhoenacker P, Haegeman G, Leysen JE. «5-HT7 receptors: current knowledge and future prospects.» *Trends Pharmacol.Sci.*, 2000: 21: 70-77.

Varin T, Gutiérrez-de-Teràn H, Castro M, Brea J, Fabis F, Dauphin F, Aqvit J, Lepailleur A, Perez P, Burgueno J, Vela JM, Loza MI, Rodrigo J. «Phe369(7.38) at human 5-HT7 receptors confers interspecies selectivity to antagonists and partial agonist.» *British Journal of Pharmacology*, 2009: 159, 1069-1081.

Vilardaga, JP. "Switching modes for G protein-coupled receptor activation." *Nature Chemical Biology*, 2006: Vol 2, No. 8, 395-396.

Weiss J, Morgan P, Lutz M, Kenakin T. "The cubic ternary complex receptor-occupancy model." *Journal of Theoretical Biology*, 1996: 178, 151-167.

Willins DL, Berry SA, Alsayegh L, Backstrom JR, Sanders-Bush E, Friedman L, Roth BL. «Clozapine and other 5-hydroxytryptamine-2A receptor antagonists alter the subcellular distribution of 5-hydroxytryptamine-2A receptors in vitro and in vivo.» *Neuroscience*, 1999: 91: 599-606.

6 APPENDIX

6.1 Abbreviation

AC	adenylyl cyclase
AMP	adenosine-3',5'-cyclic monophosphate
ATP	adenosine-5'-triphosphate
ADP	adenosine-5'-diphosphate
βAR	β-adrenergic-receptor
BSA	bovine serum albumin
cAMP	adenosine-3',5'-cyclic monophosphate
cDNA	complementary DNA
5-CT	5-carboxamidotryptamine
DNA	deoxyribonucleic acid
DMEM	Dulbecco's modified Eagle's medium
dNTP	deoxyribonucleosidetriphosphate
GPCR	G protein-coupled receptor
G protein	guanine nucleotide-binding (regulatory) protein
GTP	guanosine-5'-triphosphate
GDP	guanosine-5'-diphosphate
h	human
HEK	HumanEmbryonic Kidney 293
5-HT	5-hydroxytryptamine
IP_3	inositol triphosphate
PCR	polymerase chain reaction
PBS	phosphate buffer saline
PKA	protein kinase A (cAMP-dependent protein kinase)
PKC	protein kinase C
PLC	phospholipase C
TMH	transmembrane helix

Acknowledgements

Catania, December 2011

Agata Antonina Rita Impellizzeri